Numerical Simulation of Green Water and Resulting Loads

By

Kai Zhang

Submitted for the Degree of Master of Philosophy

Department of Naval Architecture & Marine Engineering

University of Strathclyde

September 2012

Declaration of Authenticity and Author's Rights

This thesis is the result of the author's original research. It has been composed by the author and has not been previously submitted for examination which has led to the award a degree.

Signed:

Date:

ACKNOWLEDGEMENTS

I wish to express my limitless thanks to my supervisor Professor Atilla Incecik, Head of the Department of Naval Architecture and Marine Engineering, University of Strathclyde. The thesis cannot be finished successfully without his special instruction, regular and patient help. After one-year training and education, it is only my fault if I still cannot understand so many things.

Thanks are also given to Dr. Xinqiu Gao, Dr. Li Xu and Dr. Zhiliang Gao for their very helpful discussion and moral support during my research period at the University of Strathclyde. Meantime, I should thank my friends Wei Jin and Saishuai Dai who gave me advices and helped me when I was learning Fluent software.

A warm thank is sent to Thelma Will who takes care of me as a mother. I can never forget her brilliant smile because it can make me more confident and optimistic in numerous occasions.

I also would like to express my heartfelt gratitude to my parents for their financial support and continuous encouragement and to my girlfriend Xiuming Zhao who supported and encouraged me throughout the research.

Finally, I offer my regards and wishes to those people who supported me in any aspects of study during completion of my thesis.

Abstract

The green water problem has been noted many years ago in the field of ship and marine engineering since it may have severe consequences on the ship structure. When green water incident happens, the water on the deck will hit even destroy the structures on deck. Especially in recent years, it occurs frequently and leads to many accidents related to deck bow and deck superstructures' damage of Floating Production Storage Offloading (FPSO). Therefore, the green water problem has become one of the important areas of research internationally.

Green water is one of the strongly nonlinear ship-wave interaction problems and it is very difficult to solve mathematically. The physical phenomena of the green water occurrence are very complicated. The past investigations can only describe the phenomena to some extent, cannot give a reasonable explanation for the mechanism of green water and cannot be used in engineering practice. At present, with the development of high-speed computers and advances in computational fluid dynamics, numerical simulations are carried out for forecasting and analysing nonlinear fluid motions and resulting loads as well as physical experiments. Therefore, taking full advantages of advances in numerical modelling and combining model tests with numerical modeling to solve green water problem is a promising research area.

A comprehensive review of the recent research investigations and progress made on green water problem is carried out in the present thesis. Green water flow and its impact load on the deck structure for a stationary FPSO and a moving FPSO with heave and pitch motions are investigated by a 2-D numerical simulation method. The simulations are carried out using a commercial software ANSYS FLUENT, to obtain

an FPSO motions based on the potential flow theory and realized by dynamic mesh method. The green water flow behaviour and the resulting impact loads on the deck structure are calculated and analyzed for both fixed and moving FPSO. Numerical results of fixed FPSO agreed well with the corresponding experimental ones, and the moving FPSO's results showed that ship motions have great influence on green water phenomenon. Therefore, the method developed in this study can be applied to predict the impact forces on stationary structures in waves due to green water and conduct initial research on green water problem for moving FPSOs. It also can be regarded as a good engineering approach to evaluate the green water effects. Meanwhile, it can be used for the optimization of ship lines, especially forward lines and structural design of the deck structure. It can also help to take measures to avoid the possible damages due to green water.

Key words: green water, CFD, potential flow theory, numerical wave tank, ship motion, dynamic mesh

CONTENTS

CHAPTER 1

Introduction

1.1 Green Water Problem

Ships or offshore structures are subjected to various environmental forces such as waves, wind and current when travelling in open sea. All of these forces combined together unfavorably may lead to serious motions of a ship or an offshore structure, which may result in very high forces that could cause serious damage.

Green water (also called water on deck or shipping water) problem has been considered as an important aspect for the safety and manoeuvring of ships and offshore structures for a long time in maritime world. The problem occurs everywhere along the hull, usually in a rough-sea condition, when the incoming waves exceed the freeboard and water comes onto the deck. The most severe situations are always located in the region of the ship bow in head-sea conditions. The picture in figure 1.1 (accessed from http://bobandlois.net/sailor/shippics.htm) shows the green water over the bow of a US Navy ship when it headed to Frisco, December 1955.

Figure 1.1 Example of green water

Green water is one of the strong nonlinear interaction problems between a ship and waves. Therefore, the problem is very complicated and difficult to solve. It can be divided into four separate stages to be studied. These stages as stated in Greco & Faltinsen's (2000) are "1) The run-up of the water at the bow, 2) the water shipping on the deck, 3) the subsequent flow developing along the deck and 4) the impact on ship equipment or deck house". These stages are strongly connected with each other and it is difficult to make a strict distinction amongs them. Many researchers studied some of these stages separately to get the preliminary understanding of the phenomenon.

When most green water incidents happen, the water on the deck does not lead to serious consequence and it will run off the deck. However, when plenty of water comes onto the deck, with the increase of the speed, the flow will hits various items on deck such as ship equipment, cargo and superstructure. Moreover, the huge pressure due to water impacting upon equipment and superstructure may lead to localized structural damages. More dangerous situations may lead the loss of

longitudinal strengthen of a ship or capsizing. Therefore, Tan (1969) pointed out that the measures such as reducing the operation speed and changing the course can be adopted in order to avoid green water incidents for normal merchant vessels.

1.2 Historical Developments

1.2.1 Theoretical Research

Water on the deck is a strongly nonlinear problem due to the interaction between the ship and waves. Previously, researchers focused on model tests to study green water problem. Recently, advances in numerical predictions have been made with the development of approximate numerical computational methods.

Combining the probabilistic analysis (Ochi, 1964) and the linear seakeeping analysis is a conventional way to analyze the occurrence of water on deck. The relative vertical motion between a ship and waves is an important parameter in green water problem. If the relative motion varied with the time is a random process, the green water is a statistical problem of threshold-crossing. The threshold-crossing value is the freeboard magnitude. Vermeer (1980) presented that green water occurrence must satisfy two premises: 1) freeboard exceedance larger than zero, 2) normal resultant velocity in observation point also larger than zero.

In a harsh environment, ship motion, relative motion and drift force on offshore structures are the nonlinear functions of wave height. The results calculated by the application of traditional linear computation and probabilistic method could be hugely different from actual situation. The way to improve the prediction method is to combine appropriately experimental measurements and nonlinear analysis. For

instance, hypothesizing that the time history of autocorrelation function in survival conditions approaches Gaussian random process, Drake (2000) calculated the exceedance probabilities of a slender stationary vessel experiencing long-crested waves and refined the wave surface profiles by using a second-order correction in order to estimate the nonlinear relative motions accurately.

Many aspects of green water phenomenon such as flow on the deck and impact loads cannot be described and calculated due to the limitations of traditional seakeeping analysis methods; therefore, numerical models of potential flow theory and Boundary Integral Method were applied to study the green water problem. Goda et al. (1976) came up with a dam-breaking model to simulate the flow on the deck. Later, Burchner (1995a, b) further developed it, applied it to the green water research concern with the hydrodynamic design of FPSOs and gave the expression of pressure on the deck as follows:

$$P = \frac{d(\rho h W)}{dt} + \rho g h \cos\theta \qquad (1\text{-}1)$$

Where, h is water height on the deck, W is the vertical velocity of the deck, θ is pitch angle.

Greco et al. (2000) investigated the two-dimensional impact of the water on a rigid vertical superstructure simplifying the initial conditions by using the flow characteristics similarly in a dam breaking phenomenon. In the first stage of the impact against the wall, the flow was regarded as a wedge of fluid impacting the structure. Since the gravity has a minor role, using zero gravity similarity solution, the pressure distribution along the vertical wall was calculated by a full nonlinear numerical method.

To overcome the limitation of shallow-water assumptions, a numerical simulation of

green water flow on the deck was carried out by Yilmaz et al. (2003) using non-linear dam breaking theory. Semi-analytical method, whose advantage was less CPU time-consuming compared with numerical method based on Navier-Stokes equations, was selected to solve the nonlinear dam-breaking problem. In their simulation, a jet like formation in the front of dam was similar to observations reported by Stansby et al. (1998).

In the meantime, because of computational efficiency and numerical precision of Boundary Integral Method, some researchers like Burchner & Cozijn (1997), Faltinsen et al. (2002) applied it to fluid field computation before the free surface breaking occurs. However, the simulation of green water by using the methods mentioned above including potential flow models and Boundary Integral Method is not very comprehensive and exact, because 1) the viscosity of fluid is ignored; 2) they only modelled the flow field within deck stringer.

During the last few years, some exact numerical methods such as Marker and Cell (MAC), Volume of Fluid (VOF) and Smoothed particle hydrodynamics (SPH) have been introduced to solve large deformation problem of the free surface. Through continues development, parts of these computational methods and techniques have now been incorporated in CFD software. With the development of high-performance computers, numerical simulation of green water phenomenon became possible.

Pham (2005) simulated the green water phenomenon of the S175 high-speed containership with CFD software and obtained the impact loading acting on the deck. Based on CFD software, he developed a new dam-break model with trapezoidal volume of full of water and with initial velocity to simulate the water flow on fixed deck after green water occured. For the vertical deck pressure and horizontal loading,

it was found that the time history of pressure, peak load and pressure trend got from new model matched well with experimental data; however, the result obtained from conventional dam-breaking model were much lower than experimental data. Therefore, the new model was more suitable for simulation of green water of high-speed vessel in head sea conditions. However, in the calculations, the deck was assumed to be stationary and the effect of ship motions could not be considered in his green water analysis. Thus, the prediction of vertical deck pressure can be improved by considering the deck acceleration and its relevant pressure component.

Fekken (1999) described the fluid flow on deck by using the complete Navier-Stokes equations and studied the prediction of green water by a numerical simulation program called ComFlo. Comparison between the results of the simulation and model experiment performed by MARIN showed that the global physical behavior of the water on the deck such as contours of waterfront were similar. The high velocity water "tongue" was observed both in the test and in the simulations. Although there were some differences between the tests and the simulations, the green water loadings on different structures and on the deck measured in the simulations and experiments were close. The differences are caused by numerical noise and physical differences. Similarly with the Pham's method, the motions of ships and wave field around the ship need to be taken into account in the future.

Yamasaki (2005) conducted the numerical simulation of green water on a rectangular box in regular waves. In his simulation, the modified Marker and Cell (MAC) algorithm and the density function method were used to deal with the free surface in the framework of a locally refined overlapping grid system that was employed. There are two advantages of his method: 1) the application of locally refined grids around floating body to work out the nonlinear phenomenon like roll waves as well as

breaking waves and to capture pressure peak; 2) introduction of the rigid body motion equations and the establishment of a moving grid system in a fixed global grid system to simulate the motion of floating body caused by hydrodynamic forces. The predicted impact pressure on the deck of a floating body without vertical wall agrees well with the experimental values; however, the pressure on the deck of the floating body with vertical wall only shows a similar trend with the experimental measurements. There is a lack of validation for the floating body motions.

Applying Navier-Stokes solver in combination with a free surface capturing scheme called volume-of-fluid (VOF) method; Nielsen (2004) used a two-dimensional and three-dimensional analysis to model the green water event for a fixed vessel and moving vessel respectively. The ship motion (vertical direction) was calculated by the linear wave theory in advance to determine the relative motion of the ship bow which is the result of heave and pitch motion. The computed results of the fixed ship revealed a perfectly good agreement with experimental data; the results obtained from the ship-wave interaction analysis for a moving ship based on both two-dimensional and three-dimensional methods do not correlate well with the experimental measurements.

In Touze's (2010) method, both two-dimensional and three-dimensional numerical simulations of fluid behavior on a ship's deck were investigated using a parallelized SPH code called SPH-flow. The time histories of water height on the deck based on both methods were obtained. Through comparisons with the experimental results, it was found that SPH was a good method to predict the green water flooding period and peak amplitude in two-dimension simulation. However, the comparisons between the wave heights obtained from experimental measurements and those obtained from three-dimensional SPH simulations showed that the predicted values

of maximum wave height were more than twice as much as the measured results in experiments. The difference was caused by coarse resolution due to the decrease of computational expense. Moreover, it was a pity that the author did not study the green water loading on the deck.

1.2.2 Model Experiments

For current numerical methods which are employed to resolve green water problem, their accuracy needs to be verified by experimental measurements before they are applied to simulate the green water problem.

Buchner (2000) carried out a series of green water tests in MARINTEK. A scaled ship model corresponding to full-scale ship's length, beam, draft and depth are 260.3 meters, 47.1meters, 10.5meters and 16.5 meters respectively was used during the tests. Meanwhile, different bow flare angles (0 degrees, 10 degrees, 30 degrees and 50 degrees) were applied in his tests. For the test environment, the water depth at full scale was 150 meters, and the tests were carried out in regular as well as irregular waves. In his experiments, Bucher studied the non-linear relative motions between the ship and waves, the water flow on the deck and impact pressure upon deck structures. The relationship between water height, flow velocities, impact loading on the deck and bow shape was investigated.

The results of the tests revealed that the flow patterns on the deck in his tests and those of dam-breaking simulations were very similar , and that the bow shape as well as flare angles had a significant effect on the flow on the deck. With the increase of the bow flare angles, the water height experienced a decreasing trend; however the velocity of water flow increased. As the green water impact loading is a function about water height and velocity on deck, there is a complicated relationship between

bow shape and impact loading.

In addition, according to the results of tests, the water height on the deck was proportional to the freeboard exceedance and the velocity on the deck was proportional to the square root of the freeboard exceedance. This was in accordance with the conclusion derived from dam-breaking theory. The peak force per meter breadth F_{peak} can be expressed as $F_{peak} = \rho H u^2$(ρ is the density of the water, H is the water height, u is flow velocity). Therefore, the impact loads on structures are proportional to the square of freeboard exceedance.

The probability of green water occurrence for different Froude numbers (0.1, 0.15, 0.2, 0.278 and 0.3 respectively) and varying wave frequencies was investigated by Hamoudi and Varyani (1998) by using model tests. The model of S175 high-speed containership whose scale ratio is 1/70 was chosen in their test. The number of green water occurrence and the magnitude of longitudinal impact pressure forces were recorded in the experiments. The relative motion between the ship and waves was approximated by the vessel forward speed and the wave celerity to simplify the formulation.

Experimental results indicated that freeboard height was the main factor influencing the probability and the number of green water occurrence, other factors like vessel forward speed, significant wave height and characteristic wave period also had effects on them. In terms of the green water loading, the impact pressure in longitudinal direction cannot be described by a Gaussian process and there did not exist linearization between it and regular waves; however, it can be regarded as a contribution of the momentum of shipping water, the vessel forward speed and the level of freeboard exceedance.

Stansberg and Karlsen (2001) also conducted model tests with an FPSO in MARINTEK to study the green water loading. The full-scale ship was a monohull ship with displacement of 100,000 tons and length of 200 meters. A 1/55 scale model was moored 10-line catenaries at the center of the basin. The corresponding full scale water depth was 84 metres. During the tests, the model was mounted with four different bulwarks (0.00 meter, 1.65 meters, 3.10 meters and 4.40 meters height in full scale). In the tests, there were 10 water level gauges on the deck of the bow to measure the water level and 4 wave height gauges were installed in the front bow whose function was to record the relative motion between ship bow and waves. Three load panels on the deck house wall and five load panels on the upper part of the bow were installed to measure wave loading on the deck.

The conclusions obtained from the experiments were: 1) the estimate of ship motion using linear theory was precise enough except in extreme sea states, 2) the wave overtopping and green water occurrence were, to a large extent, due to steep and energetic nonlinear waves, 3) steep waves led to highest velocities, for instance, when the water comes onto the deck, the velocity of the flow on the deck was 8~9m/s, after a short time, it increased up to about 15m/s, 4) the bulwark height had decreased the effect of the overtopping water.

A series of model tests with a FPSO in different wave periods and wave heights were carried out in MARINTEK by JuChull Han (2003) to investigate the physics of green water. In the experiments, a 1/50 scale model of the FPSO was used. To record the water level on the deck and wave disturbance around the bow, six wave probes were placed on the deck and four relative-wave elevation gages were fixed along the bow. Meantime, two load panels were also fixed on the vertical wall to measure the impact

loading. An optical recording system and continuous video recordings were used to monitor ship motions and green water phenomenon.

From this experimental study, the following conclusions were drawn: Firstly, it was found that some hypotheses used to study the green water problem by some previous researchers were invalid. For example, the pressure on the deck does not consist of only hydrostatic term. Additionally, the run-ups vary with the wave period and height. Finally, there are three stages including an impact stage, a quasi-static load stage and a plunging water stage for the green water loads acting on the superstructure.

1.3 Present Study

The aim of the present study presented in the thesis is to investigate the green water phenomenon accurately using a suitable numerical method. During the study, it was concluded that the physical phenomena can be simulated and the loads on the ship structure caused by green water can be predicted by using the method developed. In chapter one, the background and significance of the research on green water and resulting loads including development history of numerical model developments and experimental studies are reviewed in detail. In chapter two, the seakeeping problem is introduced and the mathematical model selected to resolve the ship motions in waves is described. The heave and pitch motions of a barge were calculated by using a theoretical method and ANSYS AQWA software. In chapter three, the mathematical model and the numerical method used in this research are described. In chapter four, a numerical wave tank was established based on continuity and Navier-Stokes equations. The functions of wave making and absorption were realized by adding source terms and damping function respectively, and the Volume

of Fluid (VOF) method was adopted to capture the free surface. In chapter five, a 2-D numerical model based on ANSYS FLUENT software was applied to study the green water for a fix FPSO and the comparison with Gerco's (2001) experiments was also carried out. The simulations carried out displayed a strongly nonlinear phenomenon due to ship-wave interaction. In chapter six, the ship motions were considered in the simulation to study the green water. The influence of ship motions' on green water loading was also studied through comparing the results obtained from the free FPSO and those obtained from the fixed FPSO.

CHARPTER 2

Prediction of Ship Motions in Waves

The prediction of ship motions in waves is the basis of green water occurrence research. Ship motions are important parameters for calculating freeboard exceedance and water entry velocity which are two significant conditions leading to green water occurrence. In the present research, the effect of green water on ship motions was not considered; therefore, the ship motions are predicted based on linear potential flow theory by using ANSYS/AQWA.

2.1 Formulations of the problem

2.1.1 Co-ordinate systems

It is convenient to consider three co-ordinate systems when we deal with the 3-D ship motions. One of them is the o_0-$x_0y_0z_0$ co-ordinate system fixed in flow field whose o_0-x_0y_0 plane coincides with the still-water surface and o_0-z_0 axis is directed vertically upward. In this system, the waves can be expressed conveniently. The other o-xyz is taken to be fixed in the ship which moves with the ship. The o-xy plane coincides with the still water surface when the ship stays at the equilibrium position; the o-xz plane coincides with the longitudinal plane of symmetry and o-z axis is directed vertically upward and pass through the center of gravity of the ship. The third co-ordinate system o'-x'y'z' coincides with the co-ordinate system o-xyz when the ship stays at the equilibrium position and it will not move with the ship. If

the ship moves forward with a given speed, the co-ordinate system will move forward with the same speed. The aim of the ship motions' theory is to find the mutual relationship between these sets of co-ordinate system. The figure 2.1 shows these co-ordinate systems. For a ship in waves, we can model a six degrees of freedom system to predict the rigid body's heave, sway, surge, roll, pitch and yaw motions.

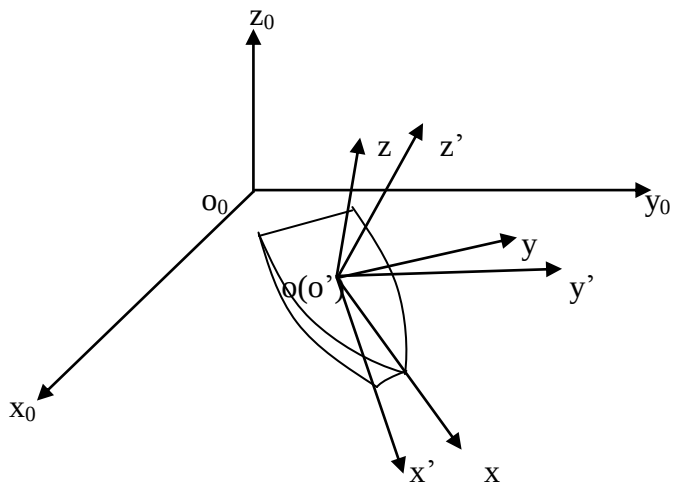

Figure 2.1 The co-ordinate systems

2.1.2 Expression of velocity potential and boundary conditions

For ship motions in waves, the total velocity potential $\Phi(x,y,z,t)$ consists of the time independent potential $[-Ux+\Phi_s(x,y,z)]$ and unsteady time dependent potential $\Phi_t(x,y,z,t)$ according to the linear potential theory.

$$\Phi(x,y,z,t)=[-Ux+\Phi_s(x,y,z)]+\Phi_t(x,y,z,t) \qquad (2\text{-}1)$$

Where, U is the forward speed of the ship.

Considering a water depth h, we assume that the velocity potential, the wave elevation and the pressure in any point are $\Phi(x,y,z,t)$; $\eta(x,y,z,t)$ and $p(x,y,z,t)$ respectively. According to the definition of velocity potential, there is a relationship

between the velocity vector of fluid particle and velocity potential,

$$\vec{V} \equiv (u, v, w) = \nabla\Phi \tag{2-2}$$

The pressure $p(x, y, z, t)$ can be derived by Bernoulli equation,

$$p - p_0 = -\rho g z - \rho\frac{\partial\Phi}{\partial t} - \frac{1}{2}\rho|\nabla\Phi|^2 \tag{2-3}$$

In the whole fluid domain, the velocity potential should satisfy Laplace equation,

$$\nabla^2\Phi = \left(\frac{\partial^2}{\partial x^2} + \frac{\partial^2}{\partial y^2} + \frac{\partial^2}{\partial z^2}\right)\Phi = 0 \tag{2-4}$$

The whole fluid domain is made up of the sea bed, the free surface, body instantaneous wetted surface and control surface at infinity. Besides Laplace equation, the velocity potential should also satisfy other boundary conditions such as linear free surface condition, body boundary condition, sea bed condition and radiation condition at infinity.

2.1.3 Evaluation of the hydrodynamic force

Before we establish the ship motion equation, we should analyze the external force acting on the ship hull. These forces mainly include wave exciting forces, rigid-body induced acceleration and velocity forces and restoring forces.

In order to calculate the hydrodynamics forces and moments on the ship, we should integrate the pressure over the mean wetted body surface instead of the instantaneous wetted surface, thus,

$$\vec{F}^{(d)}(t) = \iint p\vec{n}dS \tag{2-5}$$

$$\vec{M}^{(d)}(t) = \iint p(\vec{r} \times \vec{n})dS \tag{2-6}$$

Where, $\vec{n}$ is the unit normal vector of wetted surface, $\vec{r}$ is the position vector.

By substituting the pressure term in Equation (2-5) and Equation (2-6), we can obtain the total hydrodynamics force which can be divided into wave exciting force $\vec{F}_w$

and motion induced force $\vec{F}_m$.

$$\vec{F}^{(d)} = \vec{F}_w + \vec{F}_m \tag{2-7}$$

Furthermore, the wave exciting forces can be divided into two parts, one is well known Froude-Krylov force $\vec{F}_w^k$ and the other part is diffraction force $\vec{F}_w^d$,

$$\vec{F}_w = \vec{F}_w^k + \vec{F}_w^d \tag{2-8}$$

The rigid body induced acceleration and velocity forces can be expressed as follows,

$$-[A][\ddot{\eta}] - [B][\dot{\eta}] \tag{2-9}$$

Where, $[A]$ and $[B]$ are added mass matrix and damping coefficient matrix respectively.

The restoring forces can be written as

$$-[C][\eta] \tag{2-10}$$

Where, $[C]$ is the restoring coefficient matrix. More specific details can be found in Dai Yishan (1998) and Dai Yangshan et al's (2005) books.

2.1.4 Establishment of ship motion equation

According to the rigid body dynamic modeling to represent the ship motions in six degrees of freedom, we can obtain the matrix form of ship motion equations in waves as follow,

$$\sum_{j=1}^{6}\left[\left(M_{ij} + A_{ij}\right)\ddot{\eta}_j + B_{ij}\dot{\eta}_j + C_{ij}\eta_j\right] = F_i \ (i = 1, \cdots, 6) \tag{2-11}$$

Where, M_{ij}, A_{ij}, B_{ij}, C_{ij} are, respectively, the components of the generalized mass, added mass, damping, and restoring coefficient matrices of the ship. $F_i(i = 1, \cdots, 6)$ are the complex amplitudes of the exciting force and moment components.

We assume that the ship has lateral symmetry and the center of gravity is located at $(0, 0, z_G)$ in its static equilibrium position, the generalized mass matrix has the form of

$$[M] = \begin{bmatrix} M & 0 & 0 & 0 & Mz_G & 0 \\ 0 & M & 0 & -Mz_G & 0 & 0 \\ 0 & 0 & M & 0 & 0 & 0 \\ 0 & -Mz_G & 0 & I_{44} & 0 & -I_{46} \\ Mz_G & 0 & 0 & 0 & I_{55} & 0 \\ 0 & 0 & 0 & I_{64} & 0 & I_{66} \end{bmatrix} \quad (2\text{-}12)$$

Where, M is the mass of the ship, I_{ii} is the moment inertia in ith mode and I_{ij} are the products of inertia. Explicitly:

$$I_{44} = \int (y^2 + z^2)\, dM \quad (2\text{-}13)$$

$$I_{55} = \int (x^2 + z^2)\, dM \quad (2\text{-}14)$$

$$I_{66} = \int (x^2 + y^2)\, dM \quad (2\text{-}15)$$

$$I_{46} = I_{64} = \int xz\, dM \quad (2\text{-}16)$$

Here dM is the mass of an infinitesimally small structure element.

Similarly, the added mass, damping matrices and restoring coefficient matrix can written as follow:

$$[A] = \begin{bmatrix} A_{11} & 0 & A_{13} & 0 & A_{15} & 0 \\ 0 & A_{22} & 0 & A_{24} & 0 & A_{26} \\ A_{31} & 0 & A_{33} & 0 & A_{35} & 0 \\ 0 & A_{42} & 0 & A_{44} & 0 & A_{46} \\ A_{51} & 0 & A_{53} & 0 & A_{55} & 0 \\ 0 & A_{62} & 0 & A_{64} & 0 & A_{66} \end{bmatrix} \quad (2\text{-}17)$$

$$[B] = \begin{bmatrix} B_{11} & 0 & B_{13} & 0 & B_{15} & 0 \\ 0 & B_{22} & 0 & B_{24} & 0 & B_{26} \\ B_{31} & 0 & B_{33} & 0 & B_{35} & 0 \\ 0 & B_{42} & 0 & B_{44} & 0 & B_{46} \\ B_{51} & 0 & B_{53} & 0 & B_{55} & 0 \\ 0 & B_{62} & 0 & B_{64} & 0 & B_{66} \end{bmatrix} \quad (2\text{-}18)$$

$$[C] = \rho g \begin{bmatrix} 0 & 0 & 0 & 0 & 0 & 0 \\ 0 & 0 & 0 & 0 & 0 & 0 \\ 0 & 0 & A_w & 0 & -M_w & 0 \\ 0 & 0 & 0 & \nabla\overline{GM_T} & 0 & 0 \\ 0 & 0 & -M_w & 0 & \nabla\overline{GM_L} & 0 \\ 0 & 0 & 0 & 0 & 0 & 0 \end{bmatrix} \quad (2\text{-}19)$$

Here, the expression of A_{ij} and B_{ij} can be found in the ship motions and sea loads paper by Salvesen et al's(1970). Where A_w is the water plane area, M_w is the

moment of water plane, ∇ is the displacement of the ship, $\overline{GM_T}$ and $\overline{GM_L}$ are the transverse metacentric height and the longitudinal metacentric height respectively.

When all the terms in matrices given in Equation (2-11) are calculated, the equations of motion can be solved and the ship response can be obtained.

2.2 Case Study and Validation

AQWA-LINE is a computer program which calculates the linear response of a floating body or bodies in regular waves. The program may be used separately or in association with other programs within the AQWA suit. The principal analysis technique used within AQWA-LINE is Radiation/Diffraction theory. This type of analysis is usually used on bodies whose characteristic dimensions cause scattering of the incident regular waves. The calculation provides the first and second order wave loading on a floating or fixed body.

2.2.1 Model Description used in the case study

Let's consider a barge without forward speed has length L=200m, beam B=30m and draught D=15m.

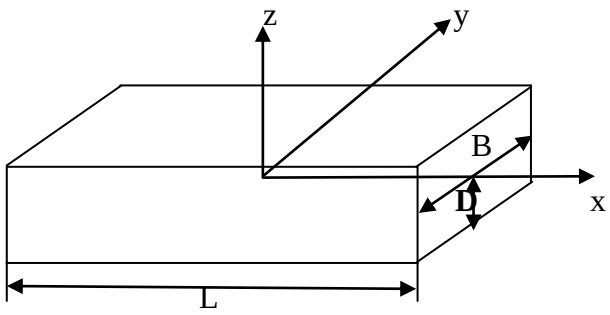

Figure 2.2 The dimensions of the barge

2.2.2 Modeling

ANSYS software is a large general-purpose finite element analysis software which is used for the analysis of structures working in fluid, electric, magnetic and sound fields. It is used to carry out a comprehensive range of engineering simulations by many companies. For modeling, ANSYS provides a complete Boolean operation and convenient as well as high-quality meshing function. Consequently, the ANSYS was adopted to establish the finite element model (shown in Figure 2.3). After that, the finite element model was converted into the .dat file and calculate the heave and pitch motions were calculated by using AQWA.

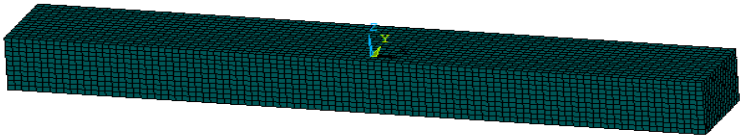

Figure 2.3 Finite element model

2.2.3 Results and validation

Figure 2.4 and Figure 2.5 show the heave and pitch RAOs computed by using AQWA. In addition, the heave and pitch motions of the barge were also calculated by using Faltisen's(1990, 2005) method. The results obtained from AQWA and those based on the Faltinsen's method matched very well as can be seen from figure 2.4 and 2.5.

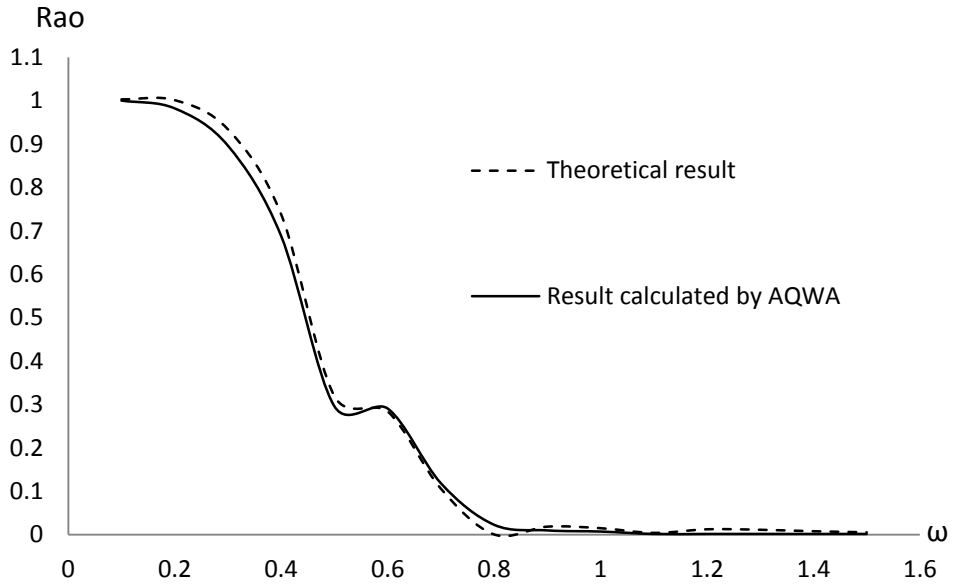

Figure 2.4 Heave motion

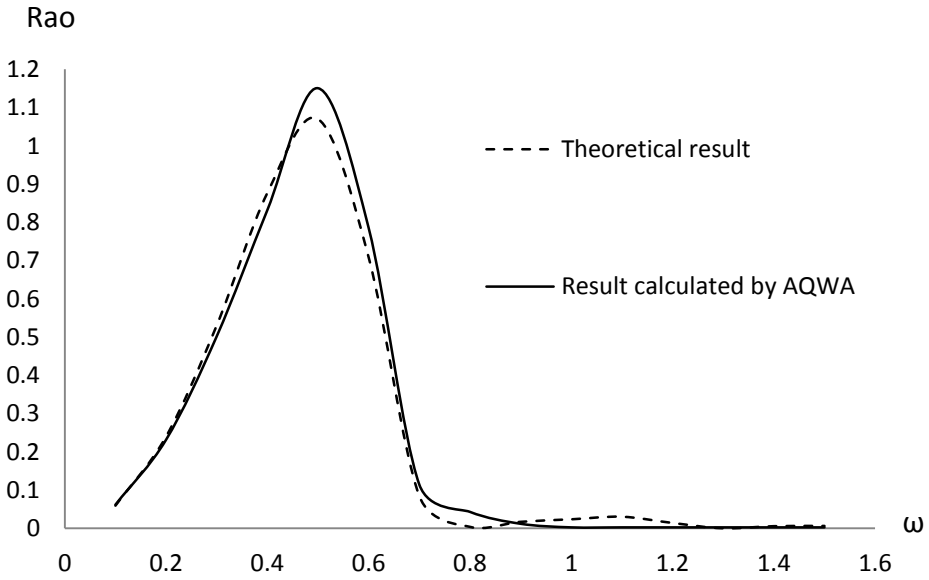

Figure 2.5 Pitch motion

2.3 Conclusions

In this chapter, ship heave and pitch motions in waves were studied. The linear seakeeping theory used is based on the assumption that the external forces acting on ships or floating bodies can be divided into three parts including wave exciting forces, rigid body induced acceleration and velocity forces and restoring forces. Once these forces are obtained, the linear motion equations can be established based on dynamics theory of rigid body.

Finally, as a case study, the heave and pitch motions of a barge were calculated by using an analytical method and ANSYS/AQWA suit of programs which are based on 3-D source distribution technique. The results obtained from the analytical method and ANSYS/AQWA correlate very well.

CHAPTER 3

Mathematical Modeling and Numerical Methodology

Green water is one of the strongly nonlinear ship-wave interaction problems and it is very difficult to solve it analytically. Consequently, the simulation of green water phenomenon was carried out by using numerical method. For the simulation of green water phenomenon, both wave-ship interaction and free surface capture are important aspects. In ANSYS FLUENT, the incompressible and compressible, laminar and turbulent fluid flow problems can be tackled conveniently due to the comprehensive modeling capabilities. At the same time, conducting the steady-state or transient simulation in ANSYS FLUENT is also available. More importantly, the set of free surface and multiphase model provided by ANSYS FLUENT provides conveniences for the simulation of green water phenomenon. Therefore, the ANSYS FLUENT software was selected in this study. In this chapter, the basic mathematical modeling and numerical methodology used in green water simulations were introduced.

3.1 Governing Equations

For all flows, the continuity equation and momentum equation are solved in ANSYS FLUENT. For the problem of multiphase flow, the Volume of Fluid (VOF) equation is adopted to capture the free surface.

Continuity equation:

$$\frac{\partial \rho}{\partial t} + \nabla \cdot (\rho \vec{v}) = 0 \qquad (3\text{-}1)$$

Momentum equation:

$$\frac{\partial}{\partial t}(\rho \vec{v}) + \nabla \cdot (\rho \vec{v}\vec{v}) = \rho \vec{g} - \nabla P + \nabla \cdot \vec{\tau} + \vec{S} \qquad (3\text{-}2)$$

VOF equation:

$$\frac{\partial}{\partial t}(a_q) + \nabla \cdot (a_q \vec{v}) = 0 \qquad (3\text{-}3)$$

$$\sum_{q=1}^{n} a_q = 1 \qquad (3\text{-}4)$$

Where:

∇	Hamiltonian or gradient operator
$\vec{V}$	Velocity vector
$\overrightarrow{\rho g}$	Gravitational body force
P	Static pressure
$\vec{\tau} = \mu\left[(\nabla \vec{V} + \nabla \vec{V}^T) - \frac{2}{3}\nabla \cdot \vec{V} I\right]$	Stress tensor
μ	Molecular viscosity
I	Unit tensor
$\vec{S}$	External body forces
a_q	Volume fraction of q-th fluid

In the VOF approach, an assumption for transported quantities is made that the field variables (velocity, pressure, temperature and turbulence quantities) are shared by all phases of fluids. Therefore, only a single set of governing equations is derived.

3.2 Numerical Methodology

In order to analyse and solve all the governing equation in ANSYS FLUENT solver

conveniently, the universal equation called transport equation is established. The transport equation for scalar quantity $\Phi\ (u, v, w, K, \omega)$ has the integral form for an arbitrary volume V as follows:

$$\int_V \frac{\partial(\rho\Phi)}{\partial t} dV + \oint \rho\Phi\vec{V} \cdot d\vec{A} = \oint \Gamma_\Phi \nabla\Phi \cdot d\vec{A} + \int_V S_\Phi dV \qquad (3\text{-}5)$$

Where:

$\vec{A}$	surface area vector
Γ_Φ	diffusion coefficient for Φ
$\nabla\Phi$	gradient of Φ
S_Φ	source of Φ per unit volume

The above Equation (3-5) is applied to each control volume, or cell, in the computational domain. The two-dimensional, triangular cell shown in figure 3.1 is an example of such a control volume. Discretization of Equation (3-5) on a given cell yields

$$\frac{\partial(\rho\Phi)}{\partial t} V + \sum_f^{N_{faces}} \rho_f \vec{V}_f \Phi_f \cdot \vec{A}_f = \sum_f^{N_{faces}} \Gamma_\Phi \nabla\Phi_f \cdot d\vec{A}_f + S_\Phi V \qquad (3\text{-}6)$$

Where:

N_{faces}	number of faces enclosing cell
$\rho_f \vec{V}_f \cdot \vec{A}_f$	mass flux through the face
$\vec{A}_f$	area of face
V	cell volume

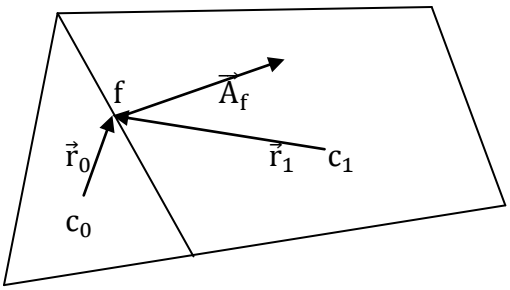

Figure 3.1 Control volume

As shown in the above Equation (3-6), there are four terms: time derivative term, convection term, diffusion term and source term. The four terms should be integrated when using finite volume discretization of the equation.

3.2.1 Spatial Discretization

The default values of scalar Φ discretized within each cell are saved at the cell center in ANSYS FLUENT. However, the calculation of convection term in the discretization equation needs the values Φ_f on each face. Therefore, an upwind scheme can be used to obtain Φ_f through interpolation.

Upwinding can be explained, explicitly, that parameters in upstream or upwind of the cell along the direction of the normal velocity v_n in discretization of transport equation are used to obtain the face value Φ_f. There are a few upwind schemes (first-order upwind, second-order upwind, power law, and QUICK) for users to select in ANSYS FLUENT.

The diffusion terms in discretization of transport equation are central-differenced and are always second-order accurate.

3.2.2 Temporal Discretization

For transient simulations, it is necessary to consider the discretization of the governing equations in both space and time. Explicitly, we regard spatial discretization as the steady-state case. Meanwhile, we integrate each term in the differential equations over a time-step Δt for temporal discretization. Generally, the

time evolution of a variable Φ can be expressed as follows:

$$\frac{\partial \Phi}{\partial t} = F(\Phi) \tag{3-7}$$

Where the function of F is the sum of any spatial discretization. In this study, first order implicit discretization is applied to the time derivative in transient problem:

$$\frac{\phi^{n+1}-\phi^{n}}{\Delta t} = F(\phi^{n+1}) \tag{3-8}$$

3.2.3 Evaluation of Gradients and Derivatives

The realization of a scalar construction at the cell faces and secondary diffusion terms as well as velocity derivatives computation depends on the gradient. For a given scalar ϕ, the convection and diffusion terms in transport equations are discretized by using the gradient $\nabla\phi$. There are three methods including Green-Gauss Cell-Based, Green-Gauss Node-Based and Least Squares Cell-Based for gradients computation in ANSYS FLUENT.

In this research, the gradient of the scalar ϕ at the cell center $c0$ is computed by using Green-Gauss Cell-Based. The discretization expression can be written as follows:

$$(\nabla\phi)_{c0} = \frac{1}{v}\sum_f \bar{\phi}_f \vec{A}_f \tag{3-9}$$

Where $\bar{\phi}_f$ is the face value, and it is taken from the arithmetic average of the values at the neighboring cell centers, i.e.,

$$\bar{\phi}_f = \frac{\phi_{c0}+\phi_{c1}}{2} \tag{3-10}$$

3.2.4 Discretization of the momentum equation

Assuming $\phi = u$, the scalar transport equation can be disceretized into the

momentum equation in x-direction as follows.

$$a_p u = \sum_{nb} a_{nb} u_{nb} + \sum p_f A \cdot \hat{\tau} + S \quad (3\text{-}11)$$

Supposing that the pressure field and face mass flux are known, Equation (3-11) can be calculated easily, and the velocity field can be calculated. However, the pressure field and face mass fluxed must be calculated because they are not known in advance. In the meantime, for the pressure, the value of the pressure at the face between c0 and c1 in figure 3.1 is needed to solve Equation (3-11); however, the ANSYS FLUENT saves the pressure at cell centers. Therefore, the computation of pressure value at face from the cell values is realized by using an interpolation scheme. Since the PRESTO! (PREssure STaggering Option) scheme is available for all meshes; this scheme is selected in this study.

3.2.5 Discretization of the continuity equation

For incompressible fluids, the discrete continuity equation can be written as follows:

$$\sum_f^{N_{faces}} J_f A_f = 0 \quad (3\text{-}12)$$

Where, J_f is the mass flux through face f.

Relating to the face values of velocity $\vec{V}_n$ and through a serial of procedure in FLUENT, the face flux J_f can be written as

$$J_f = \rho_f \frac{a_{p,c_0} v_{n,c_0} + a_{p,c_1} v_{n,c_1}}{a_{p,c_0} + a_{p,c_1}} + d_f \left(\left(p_{c_0} + (\nabla p)_{c_0} \cdot \overrightarrow{r_0} \right) - \left(p_{c_1} + (\nabla p)_{c_1} \cdot \overrightarrow{r_1} \right) \right)$$
$$= \widehat{J_f} + d_f \left(p_{c_0} - p_{c_1} \right) \quad (3\text{-}13)$$

Where:

p_{c_0}, p_{c_1}	Pressure within the two cells on either side of the face
v_{n,c_0}, v_{n,c_1}	Normal velocity within the two cells on either side of the face
$\widehat{J_f}$	A function related to velocities influence in these cells

d_f A function of $\bar{a}_p$

$\bar{a}_p$ Average of the momentum equation a_p coeffocoents

3.2.6 Pressure-Velocity Coupling

To realize the pressure-velocity coupling, an extra condition for pressure can be derived from Equation (3-13) by reformatting the continuity equation. There are five pressure-velocity coupling algorithms (SIMPLE, SIMLEC, PISO, Coupled and Fraction Step for unsteady flows using the non-iterative time advancement scheme) in FLUENT. For the SIMPLE (Semi-Implicit Method for Pressure Linked Equations) algorithm, there is a relationship between the velocity and pressure corrections. Through the use of this relationship, the mass conservation can be achieved and the pressure field can be obtained. Therefore, the SIMPLE scheme is chosen.

Using a guessed p^* and resolving the momentum equation, the face flux, J^*_f can be calculated as follows:

$$J^*_f = \widehat{J^*_f} + d_f\left(p^*_{c_0} - p^*_{c_1}\right) \tag{3-14}$$

However, Equation (3-14) does not satisfy the continuity equation. Therefore, there should be a correction for J^*_f and the corrected face flux J_f can be expressed as follows:

$$J_f = J^*_f + J'_f \tag{3-15}$$

Where, J'_f is a correction. And it has a form in SIMPLE as

$$J'_f = d_f\left(p'_{c_0} - p'_{c_1}\right) \tag{3-16}$$

Where p' is the cell pressure correction.

Inserting Equation (3-15) and Equation (3-16) into Equation (3-12), Equation (3-17)

for pressure correction can be obtained as follows:

$$a_p p' = \sum_{nb} a_{nb} p'_{nb} + b \tag{3-17}$$

Where, b is the mass imbalance in control volume.

From Equation (3-17), the pressure and flux can be obtained as follows:

$$p = p^* + \alpha_p p' \tag{3-18}$$

$$J_f = J^*_f + d_f \left(p'_{c_0} - p'_{c_1} \right) \tag{3-19}$$

Where, α_p is the under relaxation (about 0.3).

3.2.7 Geometric Reconstruction Method

For the discretization of the volume fraction equation, special treatments are needed. Using the abnormal interpolation method (e.g. second order upwinding) will result in strong numerical diffusion because of the large volume fraction gradient near the interface (it is a discontinuous interface for volume fraction function). The geometric reconstruction scheme is an effective algorithm to capture the free surface without any loss of sharpness. For the green water problem, the free surface is normally steep at the bow and many nonlinear phenomena such as wave breaking will appear. Therefore, the geometric reconstruction scheme with VOF approach is used in this research.

In the geometric reconstruction scheme, a linear function assumption which is used to compute the advection of fluid through the cell faces is applied in each cell of the interface. Generally, there are three steps to this approach.

- According to the details of volume fraction and its derivatives in the cell, the position of the linear interface in each partially-filled cell should be calculated

firstly.

- After obtaining the linear interface’s position, the fluid fluxes through each face can be calculated according to the normal and tangential velocity distribution on the face.
- Finally, the volume fraction in each cell is calculated again based on the balance of fluxes computed during the previous step.

CHAPTER 4

Establishment of Numerical Wave Tank

The effective way to study ship performance is to conduct experiments. However, experimental studies are very expensive and time-consuming. With the rapid development of high performance computers, the researchers have recently established numerical wave tank to carry out numerical simulations instead of physical experiment. Comparing with model tests, numerical wave tank has some specific advantages such as low cost and no scale effect issues. This chapter is aimed at the establishment of an effective numerical wave tank for green water simulations.

4.1 Governing Equations and A Numerical Method

4.1.1 Wave Generation Technique

The incompressible fluid flow can be described by the continuity equation and Navier-Stokes equations

$$\frac{\partial \rho}{\partial t} + \frac{\partial (\rho u)}{\partial x} + \frac{\partial (\rho v)}{\partial y} = 0 \tag{4-1}$$

$$\frac{\partial (\rho u)}{\partial t} + u\frac{\partial (\rho u)}{\partial x} + v\frac{\partial (\rho u)}{\partial y} = \mu\left(\frac{\partial^2 u}{\partial x^2} + \frac{\partial^2 u}{\partial y^2}\right) - \frac{\partial p}{\partial x} \tag{4-2}$$

$$\frac{\partial (\rho v)}{\partial t} + u\frac{\partial (\rho v)}{\partial x} + v\frac{\partial (\rho v)}{\partial y} = \mu\left(\frac{\partial^2 v}{\partial x^2} + \frac{\partial^2 v}{\partial y^2}\right) - \frac{\partial p}{\partial y} - \rho g \tag{4-3}$$

Where u and v are the velocity component of fluid particles in the x and y directions, g is the gravity acceleration and ρ is the density.

The wave generation by introducing source function can be based on one of following methods: First method is to introduce a mass source function into the continuity Equation (4-1) inside the computational domain. Another method is to add momentum source functions in the Navier-Stokes Equation (4-2) and Equation (4-3). Combining the above two methods to generate desired waves is also another method. In the present study, the third method was used that is adding mass and momentum source functions in the continuity and Navier-Stokes equations. Therefore, the equations were modified as follows:

$$\frac{\partial \rho}{\partial t} + \frac{\partial (\rho u)}{\partial x} + \frac{\partial (\rho v)}{\partial y} = S_q \quad (4\text{-}4)$$

$$\frac{\partial (\rho u)}{\partial t} + u\frac{\partial (\rho u)}{\partial x} + v\frac{\partial (\rho u)}{\partial y} = \mu\left(\frac{\partial^2 u}{\partial x^2} + \frac{\partial^2 u}{\partial y^2}\right) - \frac{\partial p}{\partial x} + S_x \quad (4\text{-}5)$$

$$\frac{\partial (\rho v)}{\partial t} + u\frac{\partial (\rho v)}{\partial x} + v\frac{\partial (\rho v)}{\partial y} = \mu\left(\frac{\partial^2 v}{\partial x^2} + \frac{\partial^2 v}{\partial y^2}\right) - \frac{\partial p}{\partial y} - \rho g + S_y \quad (4\text{-}6)$$

Where, S_q, S_x and S_y are the additional source function and momentum source functions in x and y directions respectively. The additional source functions can be calculated by using Euler equations.

The Volume of Fluid (VOF) method was used to capture the free surface deformation. Thus, the volume fraction a_q which presents the ratio of q-th fluid was introduced. In this research, q=1 represents air phase and q=2 represents water phase. Volume fraction a_q must satisfy the equations as follows:

$$\frac{\partial a_q}{\partial t} + \frac{\partial (u a_q)}{\partial x} + \frac{\partial (v a_q)}{\partial y} = 0, \quad q = 1,2 \quad (4\text{-}7)$$

$$\sum_{q=1}^{2} a_q = 1 \quad (4\text{-}8)$$

To realize the wave generation, Wang and Liu's (2005) technique was adopted in the wave numerical simulations carried out in this study. Let's hypothesize that the velocity and dynamic pressure in the fluid domain after wave generation is:

$$\begin{cases} u_m = cu_l \\ v_m = cv_l \\ p_m = cp_l \end{cases} \tag{4-9}$$

Where, the subscript l is the theoretical value of the desired wave and $c = c(x)$ is a smoothing weighting function which varies with the x position.

In the wave making zone, the velocity and dynamic pressure must satisfy the continuity equation and the Euler equations with source terms. Therefore, we can get:

$$\frac{\partial \rho}{\partial t} + \frac{\partial (\rho u_m)}{\partial x} + \frac{\partial (\rho v_m)}{\partial y} = S_q \tag{4-10}$$

$$\frac{\partial (\rho u_m)}{\partial t} + u_m \frac{\partial (\rho u_m)}{\partial x} + v_m \frac{\partial (\rho u_m)}{\partial y} = -\frac{\partial p_m}{\partial x} + S_x \tag{4-11}$$

$$\frac{\partial (\rho v_m)}{\partial t} + u_m \frac{\partial (\rho v_m)}{\partial x} + v_m \frac{\partial (\rho v_m)}{\partial y} = -\frac{\partial (p_m - \rho g y)}{\partial y} - \rho g + S_y \tag{4-12}$$

Substituting Equation (4-9) into Equation (4-10) to Equation (4-12), the three source terms S_q, S_x and S_y can be obtained as follows:

$$S_q = \rho u_l \frac{\partial c}{\partial x} \tag{4-13}$$

$$S_x = \rho(c^2 - c)\left(u_l \frac{\partial u_l}{\partial x} + v_l \frac{\partial u_l}{\partial y}\right) + \frac{\partial c}{\partial x}\left(\rho c u_l^2 + p_l\right) \tag{4-14}$$

$$S_y = \rho(c^2 - c)\left(u_l \frac{\partial v_l}{\partial x} + v_l \frac{\partial v_l}{\partial y}\right) + \frac{\partial c}{\partial x} \rho c u_l v_l \tag{4-15}$$

For the selection of smoothing weighting function $c(x)$, it should satisfy the requirements as follows:

$$\begin{cases} 0 \le c(x) \le 1 \\ c(x_0) = 0 \\ c(x_1) = 1 \\ \frac{\partial c}{\partial x}(x = x_0) = 0 \end{cases} \tag{4-16}$$

Where, x_0 and x_1 are the starting position and ending position of wave making zone.

According to the requirements mentioned above, the smoothing weighting function

was chosen as,

$$c(x) = \sin^2\left(\frac{x-x_0}{x_1-x_0} \times \frac{\pi}{2}\right) \quad (4\text{-}17)$$

4.1.2 Wave Absorption Technique

An absorption zone is set at the end of the wave flume. It aims at the absorption of wave energy and preventing transmitted wave reflection. The function of wave absorption can be realized by adding damping function, momentum source and porous medium in the wave absorption zone. In this study, the method of adding damping function to achieve wave absorption was adopted. For this method, an artificial damping zone equal to 1-2 wave length before the open boundary to enforce the decay of waves was set.

Taking the 2-D numerical wave tank for example, the Navier-Stokes equations in wave absorption zone can be written as,

$$\frac{\partial(\rho u)}{\partial t} + u\frac{\partial(\rho u)}{\partial x} + v\frac{\partial(\rho u)}{\partial y} = \mu\left(\frac{\partial^2 u}{\partial x^2} + \frac{\partial^2 u}{\partial y^2}\right) - \frac{\partial p}{\partial x} + \gamma\rho u \quad (4\text{-}18)$$

$$\frac{\partial(\rho v)}{\partial t} + u\frac{\partial(\rho v)}{\partial x} + v\frac{\partial(\rho v)}{\partial y} = \mu\left(\frac{\partial^2 v}{\partial x^2} + \frac{\partial^2 v}{\partial y^2}\right) - \frac{\partial p}{\partial y} - \rho g + \gamma\rho v \quad (4\text{-}19)$$

Here, $\gamma = \gamma(x)$ is damping coefficient. The fluid in the wave absorption zone also needs to satisfy continuity equation.

The use of the damping coefficient of linear distribution is not good for nonlinear wave absorption. Larson and Dancy (1983) suggested that waves can be absorbed by using sponger layer and pointed out that the coefficient should be

$$\gamma(x) = \begin{cases} \exp\left[\left(2^{-x/\Delta x} - 2^{-x_s/\Delta x}\right)\ln a\right], & 0 \le x \le x_s \\ 1 & x_s < x \end{cases} \quad (4\text{-}20)$$

where x is the distance from grid point to open boundary, x_s is breadth of sponger layer, Δx is breadth of grid, a is a constant that depends on the number of grid lines

in the layer, $x_s/\Delta x$.

Although this damping coefficient can be used in nonlinear wave absorption theoretically, the sponger layer should vary with time and space. Therefore, it is difficult to achieve it.

For 2-D numerical wave tank, the same technique as used by Makoto Arai and Uttam Kumer Paul (1993) is adopted in this study. That is the reduction of vertical velocity inside the wave absorption zone. However, the horizontal velocity remains unchanged, because reduction of horizontal velocity will disturb the continuity of the flow and reflection will occur at the boundary.

$$v_s(x, y, t) = \gamma(x)v(x, y, t) \tag{4-21}$$

Where, $\gamma(x)$ is damping coefficient.

$$\gamma(x) = \alpha\left(\frac{x-x_s}{x_e-x_s}\right)^2 \tag{4-22}$$

where, α is a constant that the author calls it damping control parameter, x_s is the start point of sponger layer and x_e is end point of sponger layer.

4.2 Numerical Simulation of Waves

4.2.1 Problem Description

The significance of numerical wave tank establishment is the fact that the numerical simulations can instruct physical experiment and replace it partly. A numerical tank should have the functions of wave making and absorption, at the same time; it needs to solve the interaction between waves and a structure. The accuracy of numerical results very much depends on the accuracy of waves generated. Therefore, numerical

simulation of waves is an important module of numerical wave tank.

Figure 4.1 is the sketch map of numerical wave tank used in this study. The numerical wave tank is divided into three zones: wave making zone, working zone and transmitted wave absorption zone. The upper side of the tank is air and its lower side is water. EF denotes still water surface.

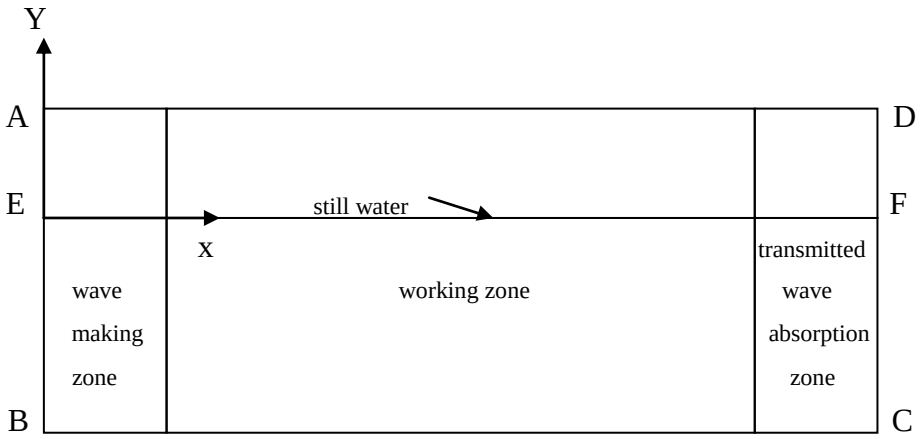

Figure 4.1 sketch map of numerical wave flume

4.2.2 Boundary Conditions and Solver Setups

In the computation domain, we should have boundary conditions set up as follows: the top boundary AD is pressure outlet; left boundary AB; right boundary CD and bottom boundary BC are all wall. In order to simulate the numerical waves, we use software Fluent to resolve the control equations (continuity equation, Navier-Stokes equations and VOF equation). Before the calculations, the free surface is calm (u=0 and v=0) with an initial static pressure distribution. Therefore, we set u=0 and v=0 as initialization conditions. At the same time, the fluid domain is simulated by using the assumption of laminar flow; the pressure and velocity are calculated iteratively by adopting a SIMPLE scheme; First Order Upwind Scheme is used in momentum equations and Geo-Reconstruct is used in Volume Fraction Discretization. Finally,

the numerical wave generation and absorption are realized through User-Defined Function (UDF) in the Fluent platform.

4.2.3 Mesh Layout

The following aspects should be considered when the meshing of a numerical tank is considered:

1. There should be enough grids in the direction of wave propagation in order to avoid reduction of wave height due to numerical damping. Similarly, more refined grids should be placed around the still water surface so that the position of free surface can be captured correctly.
2. The size of grids in different zones should vary smoothly. We should also consider the calculation time. Therefore, in the wave absorption zone, the size of grids can increase from small to large. In this way, the computing time should be saved and the waves can be absorbed quickly.
3. There should be enough refined grids near the structure in order to enhance the accuracy of computations and capture the local details of fluid domain.

According to the rules mentioned above, the mesh layout of numerical tank generated can be seen in figure 4.2. The length of grids in longitudinal direction should be 1% of wave length in wave making zone and working zone, however, the size of the grids increases from 1% of wave length to larger in the wave absorption zone. For the size of grids in vertical direction, the size should be 1/40 of wave height near the still water surface. Then the size increases gradually when the position is far away from the still water surface.

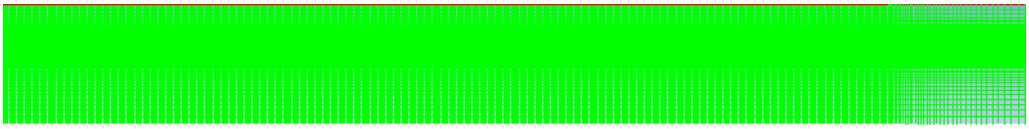

The mesh layout of the whole wave flume

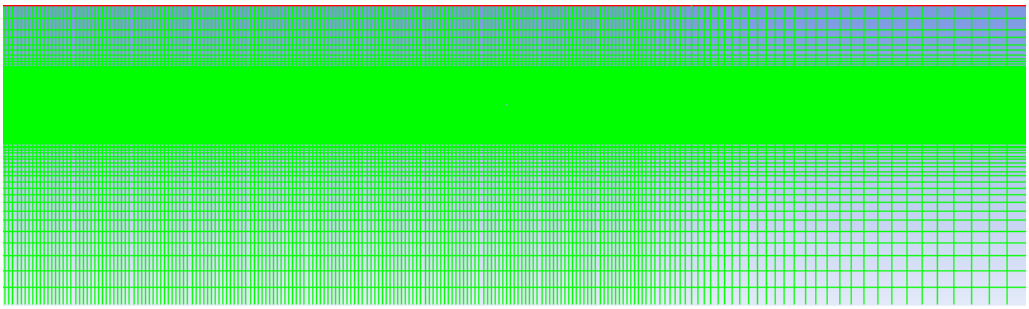

Local mesh layout of the wave flume

Figure 4.2 Mesh layout of the wave flume

4.2.4 Case Study and Results

Greco .M et al (2001) had conducted experiment to study the green water phenomenon for a fixed FPSO. For convenience, their wave tank dimensions and wave parameters were used to validate the method developed in this study. The wave tank is 13.5m long and 1.035m deep. The wave length and wave height of the desired wave are 2m and 0.16m respectively. The zone from 0m to 2m was fixed as the wave making zone and the zone from 11.5m to 13.5m as the wave absorption zone.

Adopting the method developed to realize wave making and wave absorption functions, surface elevation at x=3 as well as x=6 and the wave profile in the whole wave tank were generated and the results can be seen in figures 4.3, 4.4 and 4.5 respectively.

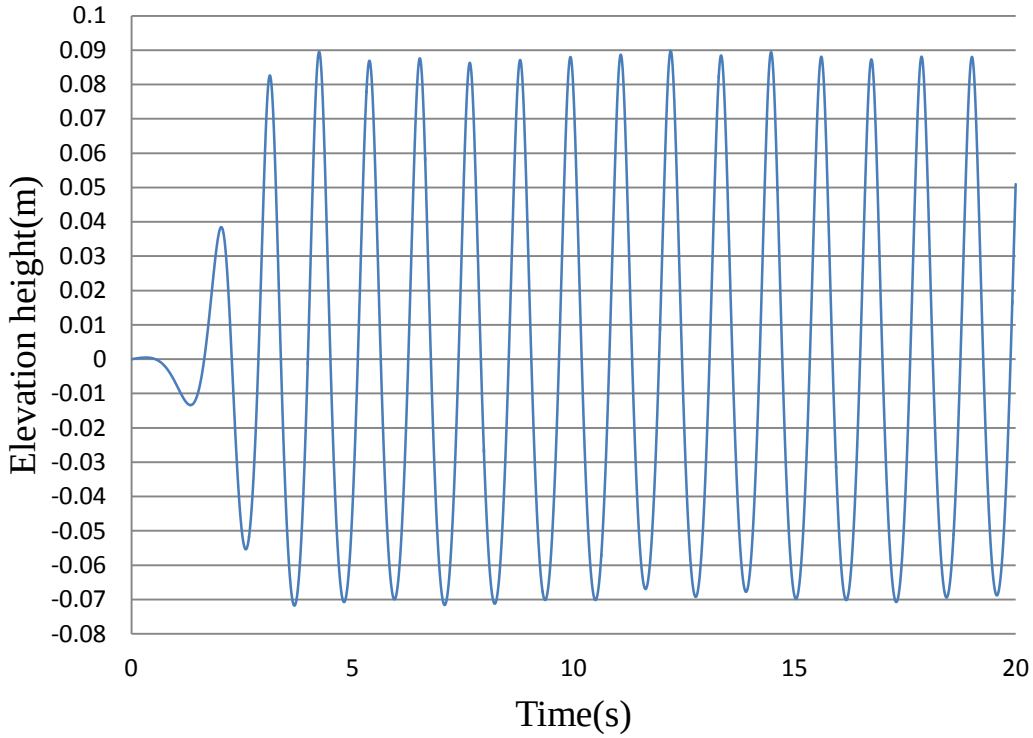

Figure 4.3 Time history of wave profile at x=3m

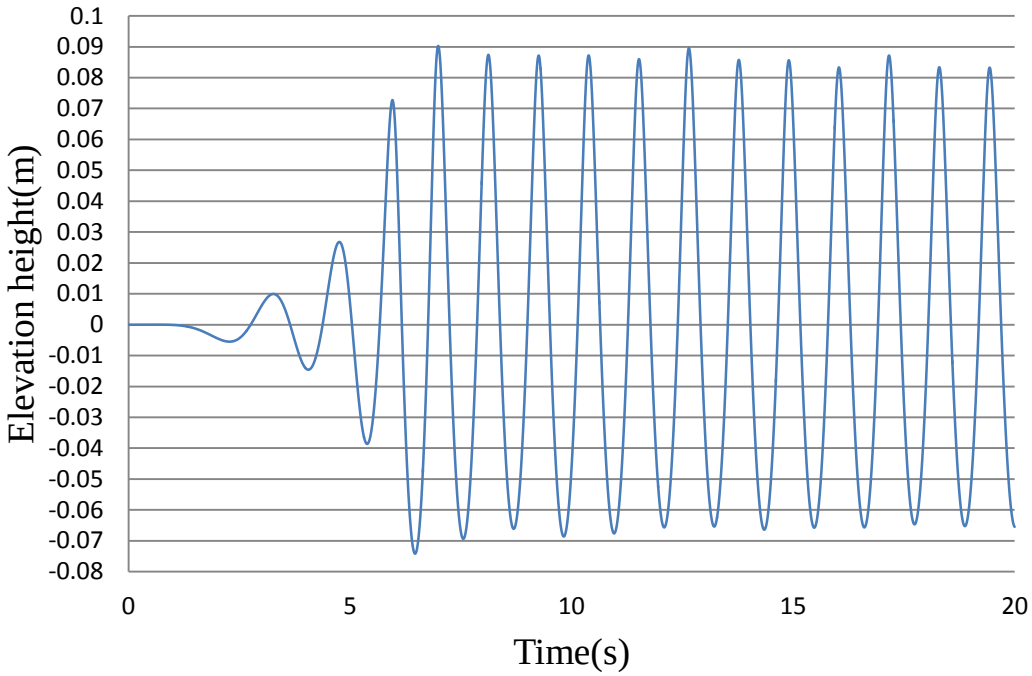

Figure 4.4 Time history of wave profile at x=6m

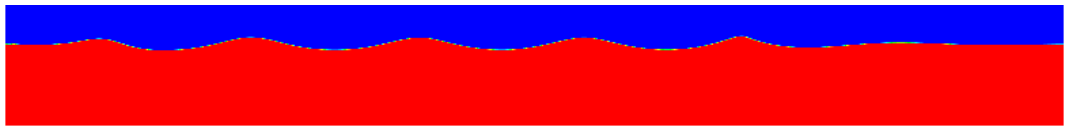

T=10s

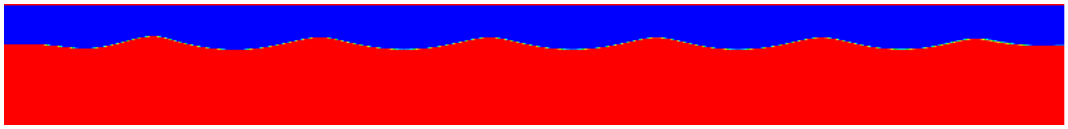

T=15s

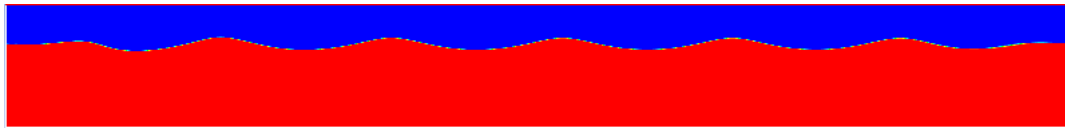

T=20s

Figure 4.5 Wave profile in the whole flume

As can be seen in figures 4.3 and 4.4, wave period is about 1.134s and the wave height is approximately 0.16m. However, the values of wave crest and wave trough remains steadily around 0.09m and -0.07m respectively. This is because the wave with length of 2m and height of 0.16m should belong to second-order Stokes wave and the nonlinear term is considered when the Fluent software calculated the wave equations. According to the formulas of second-order wave, we can get that the theoretical values of wave crest and wave trough are 0.0902m and -0.0698 respectively. Therefore, the waves generated by using the present method can be considered as good.

4.3 Conclusions

In this chapter, a numerical wave tank was established based on the CFD theory. The functions of wave making was realized by adding mass and momentum source into continuity equation and Navier-Stokes equations respectively. A sponger layer was

placed in the wave absorption zone to achieve the function of wave absorption. The numerical results show that the method developed in this study can be adopted to simulate the numerical wave tank.

CHAPTER 5

Green Water Simulation for Fixed FPSO

Floating Production Storage and Offloading (FPSO), is usually moored in specific waters to produce; store and offload oil for a number of years. They suffer greater risks than other types of vessels because they are in severe ocean environment and no operational actions can be taken to decrease the possibility of green water on deck. Consequently, there are usually several damages of green water incidents with FPSO's bow and deck structures. Ersdal & Kvitrud (2000) presented some examples of green water incidents with Norwegian FPSOs. In recent years, with the widespread use of FPSOs in the offshore industry, water on deck has been considered an important risk for FPSOs and a significant factor in ship design. Therefore, the research on green water and damages due to green water has become an internationally ongoing issue at present. However, the physical phenomenon of green water is very complicated and most of green water studies concerning FPSOs are model experiments. To validate the present method developed, we adopted Greco's (2001) experimental conditions to simulate the green water and to calculate loading due to green water.

5.1 Model Description

The two-dimensional numerical simulation of green water was carried out in the

wave tank described in chapter 4. The FPSO used in the simulations is simplified as an approximate rectangular box. Its length, height, draft and freeboard are 1.5m, 0.248m, 0.198m and 0.05m respectively; and there is a small circle (radius=0.08m) at the bow corner. According to Greco's (2001) description in his thesis, the front part of the FPSO model should be placed at 7.54m from the left boundary. The dimensions of the FPSO model and wave tank are shown in figures 5.1 and 5.2.

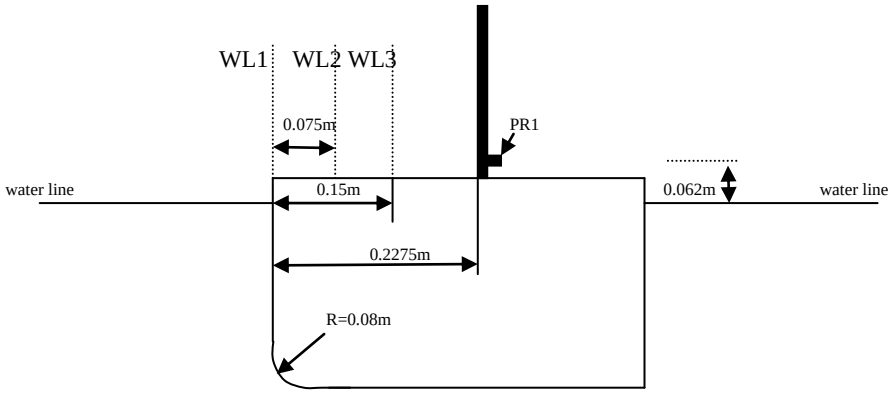

Figure 5.1 Sketch map of FPSO model

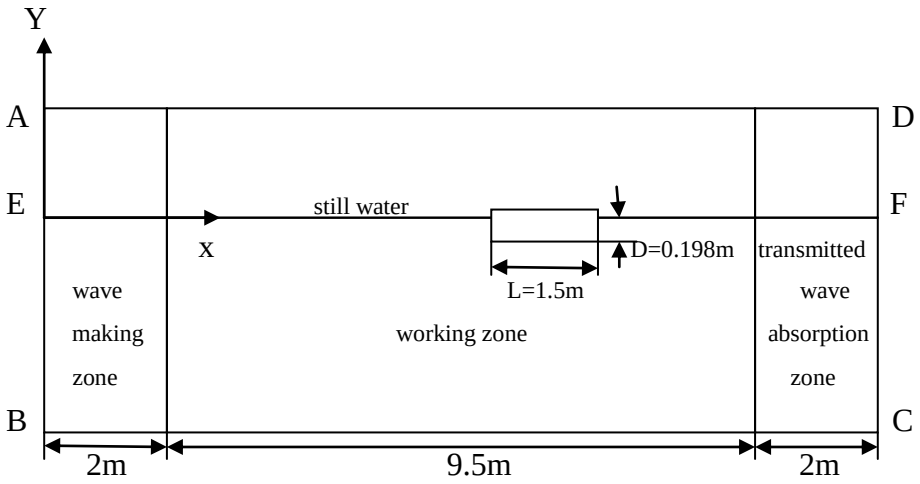

Figure 5.2 FPSO in numerical wave flume

5.2 Numerical Model

5.2.1 Mesh Layout

For the green water simulation of a fixed FPSO, besides the rules given in chapter 4, considering the interaction between FPSO and waves, we should also follow the rules given below.

1. Because of the complicacy of the fluid domain near the bow, there should be enough refined grids near the bow.
2. When wave reaches to the bow of the FPSO, it climbs along the bow; runs onto the deck; flows on the deck and hit the deck structures. Some complicated phenomena such as wave rolling and wave breaking will appear during this period. The length of the waves on the deck is smaller than the length of incident waves'. Thus, the dimension of grids around bow deck should be much smaller than outer fluid field.

The shape of structured grid is regular, its arrangement is ordered, the distort rate of geometry is small. The fitting of free surface has high accuracy in post processing by using structured grid; therefore, the structured grid is suitable for resolving the problem of wave-body interaction. Because it is very strict with the regularity of the zone's shape when the zone is meshed by using structured grids, we divided the whole domain into nine zones according to the characteristics of this problem. As shown in figure 5.3, the bow of the FPSO is in the block 5, the green water incident happens in this zone and it requires refined mesh to capture the actual physical phenomena, thus, the dimension of grids in the block 5 is smallest. The block 7, 8 and 9 are located in the end of the wave tank, these zones' function is wave absorption and there are no important physical phenomena in these zones, therefore, the dimension of grids in these zones can be much bigger. At the same time, the

numerical damping can make the function of wave absorption much better. As for the other zones, they can be meshed referring to the rules in chapter 4. Due to the different dimensions of grids in each zone, we should consider that the dimensions of grids in the adjacent area between different zones must vary smoothly in order to avoid iteration divergence and large error in the computational results. The figure 5.4 displays the mesh layout of the whole numerical flume and mesh layout around the bow of FPSO.

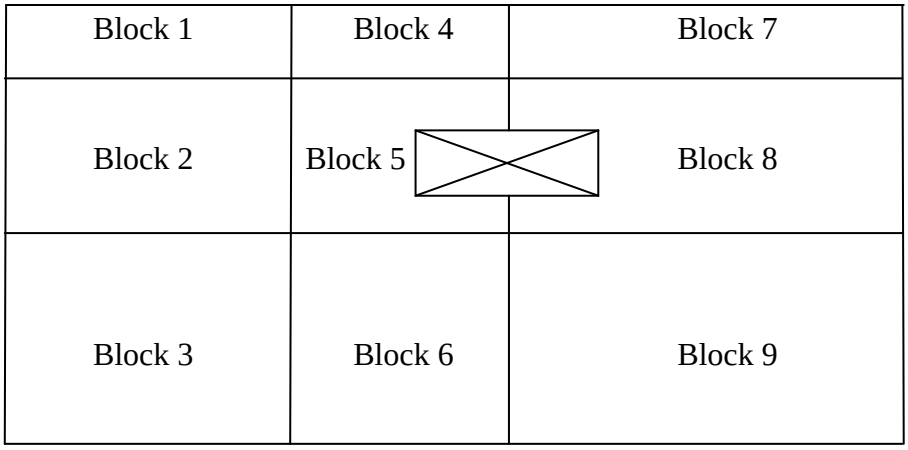

Figure 5.3 Block distribution

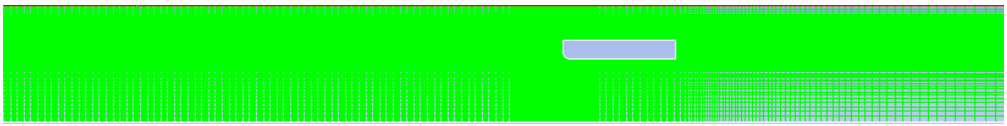

Mesh layout of the whole flume

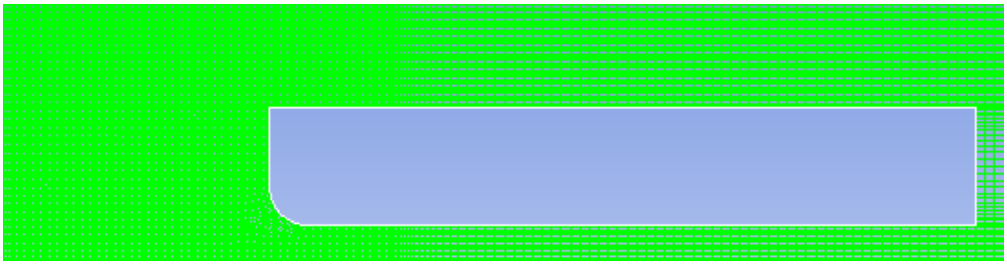

Mesh layout around FPSO

Figure 5.4 Mesh layout display

5.2.2 Boundary Conditions and Solver Setups

The same as the settings of numerical wave tank in chapter 4, the top boundary AD is pressure outlet; left boundary AB; right boundary CD, bottom boundary BC and the faces of FPSO are all wall. At initial moment, the velocities in fluid flow field are zero, and the pressure is static pressure. The laminar flow; SIMPLE scheme; First Order Upwind Scheme and Geo-Reconstruct are chosen in solver setups.

5.3 Validation and Analysis

5.3.1 Water level on the deck and impact pressure

In Greco's experiment, there were three wave probes placed at the bow and at 0.075m as well as 0.15m from the bow to measure the water elevation. Likewise, we also monitored the water elevation at these three observation points and these monitored points were named WL1, WL2 and WL3. Figures 5.5, 5.6 and 5.7 give the results of present simulations, the experimental results and Zhu's (2009) simulation results. As can be seen from the comparison, they match very well and present simulation results are close to the experimental results. We can see that the incoming wave is steeper compared to the theoretical wave prescribed in UDF for both of the first two green water events. Obviously, there is more shipping water on the deck for the second green water event. This is because the wave crest reaching the bow steepens due to reflected waves.

As can be seen from figures 5.5, 5.6 and 5.7, the computational results obtained by using the present method coincides with the experimental results on magnitude and trend. However, the peak values obtained from calculation are a bit lower than the

experimental measurements. This is probably because the factor of viscosity is not considered in the simulation of flow on the deck. The motion of fluid should be impeded to make the fluid accumulate on the deck due to the viscosity effect. Therefore, in the same conditions, the water elevation height obtained from the experimental measurements is larger than that obtained from the numerical simulations. At the same time, the differences in wave profile between experimental measurements and present numerical simulations may cause the error at initial stage.

The impact force due to green water flow acting on the ship deck and deck structure is an important issue for navel architecture and offshore engineering. In order to get insight into this research, an FPSO with a vertical wall (shown in figure 5.1) on the bow deck was also modeled. The vertical wall is located on the fore part of the deck, 0.2275 m from the bow, and its height is 0.3m and the wave cannot overtop from the top of the vertical wall. The monitored point of impact pressure named PR1was set at a location of 12mm high from the deck on the vertical wall to collect pressure data. Figure 5.8 displays the time histories of impact pressure in one wave period obtained from present calculations, experimental measurements and Zhu's calculations. There are two significant peaks in the figure. The first peak appears at the moment when the initial impact happens, and the second peak corresponds to the moment when the water after reaching maximum height starts to run down from the wall. The results and trend obtained from the calculations and measurements are in good agreement. However, both of the two peaks values obtained from calculations are larger than those obtained from experimental measurements. The probable reason for this is also due to the fact that we did not consider the effect of viscosity. The fluid motion should not be impeded in our simulation, thus, the velocity of flow before hitting the wall obtained in the present simulations is larger than that obtained from the experimental measurements. According to Bernoulli equation, the fact that the

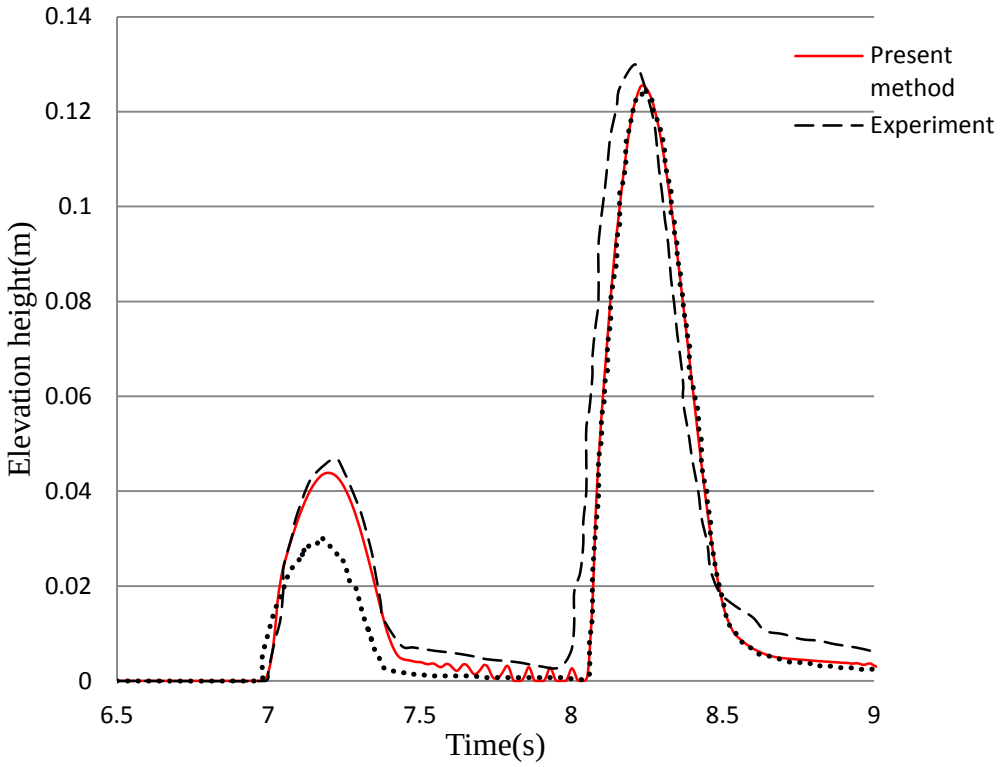

Figure 5.5 Time history of water level measured by WL1

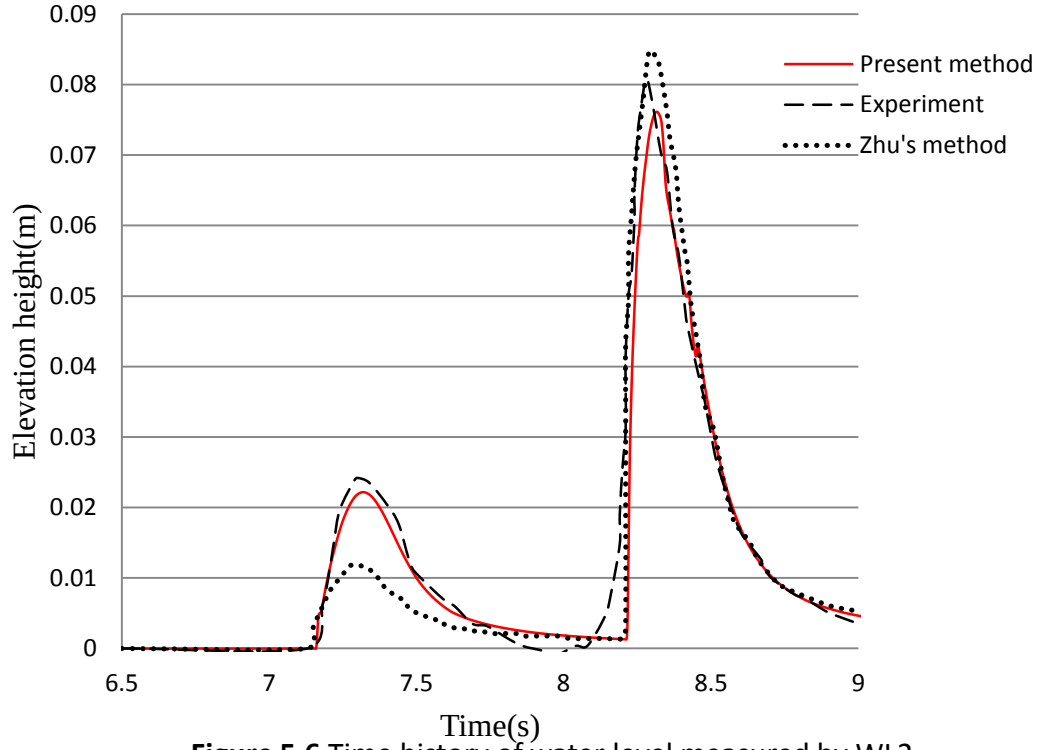

Figure 5.6 Time history of water level measured by WL2

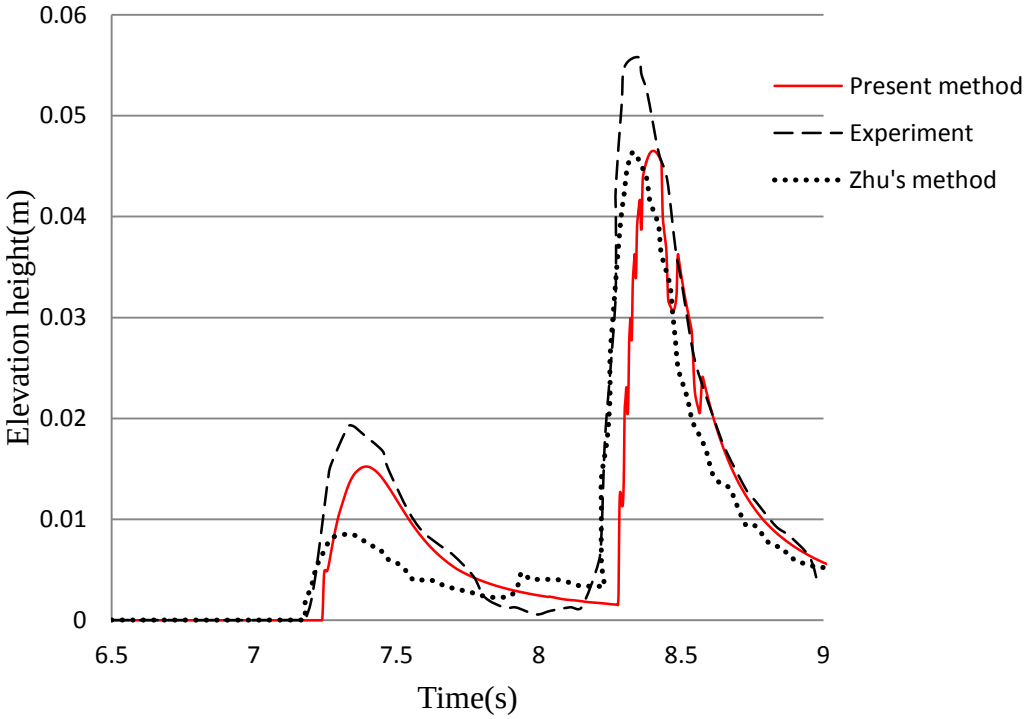

Figure 5.7 Time history of water level measured by WL3

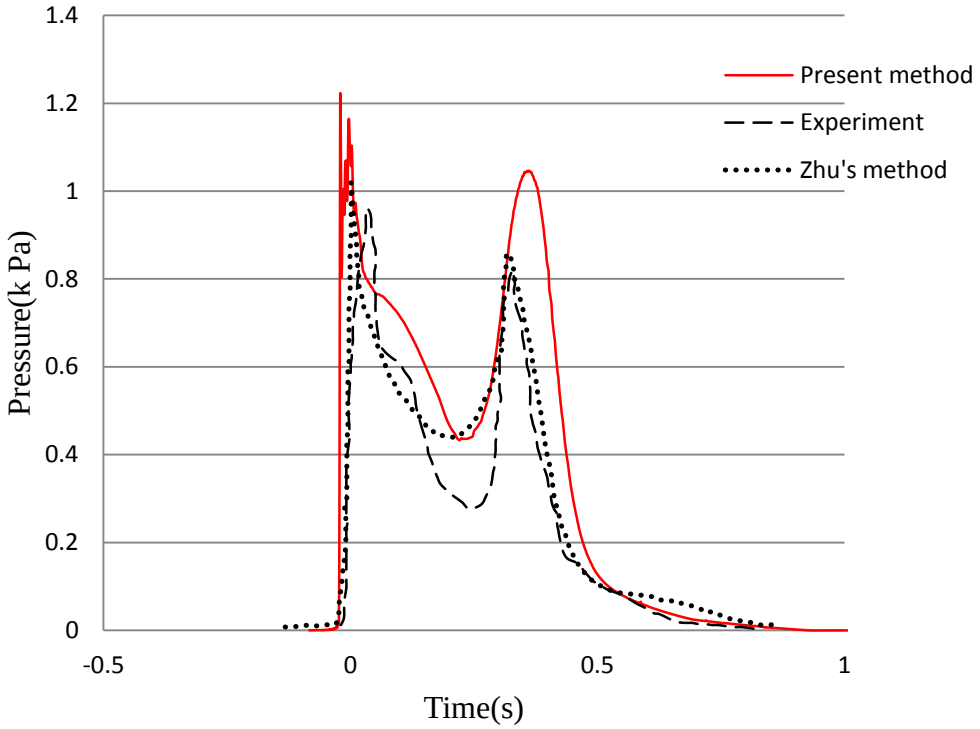

Figure 5.8 Time history of water level measured by WL2

pressure values in the present simulations is larger than those obtained from the experimental measurements is reasonable.

5.3.2 Stages of green water phenomenon

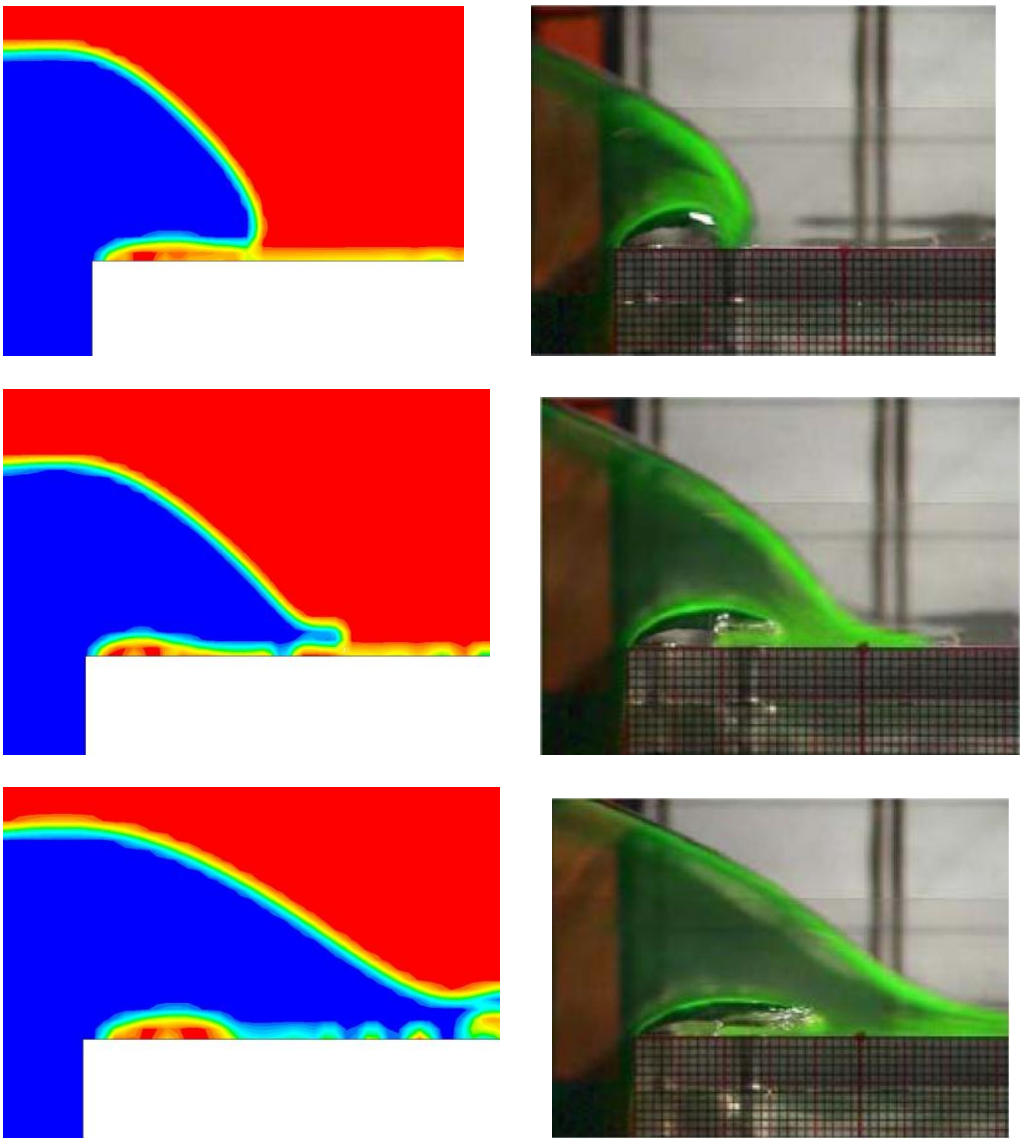

Figure 5.9 Visualization of shipping water on the FPSO deck

Figure 5.9 reveals the instantaneous images (numerical simulation on the left side and experimental results on the right side) in different stages of green water. The

numerical and experimental results are fairly close. The stages described in Greco & Faltinsen's (2000) study, two strands of jet flow after water hitting the deck and air cavity can be observed in the simulations. However, we can also found some differences in the comparisons. For example, the water height and the shape saturation of water in the numerical simulation are lower than those observed in the experiments. Probably there are two reasons leading to these differences, the first one is that the surface tension was not considered in the simulation; the second one is that the 2-D experiments were carried out in 3-D space, the factors of photographic angle as well as scope and image scale may cause the differences.

5.4 Conclusions

In this chapter, we introduced a 2-D simplified FPSO model to study the interaction between the fixed FPSO and waves in extreme wave condition. Some complicated phenomenon like wave climbing, wave breaking, impact and jet flow can be observed in the simulations. The computational results matched with the experimental measurements well, therefore, the fluid flow on the deck and the impact loading on the deck structure can be predicted successfully by using the present method.

CHAPTER 6

Initial Study of Green Water for Moving FPSO

Ship in waves will produce six degrees of complex motions: heave, sway, surge, roll, pitch and yaw. These motions have very important effects on occurrence of green water and its severity. In this chapter, considering heave and pitch motions, we focused on studying the simulation of green water for a moving FPSO in head seas. The heave and pitch motions are approximately calculated by using the method described in chapter 2. The simulation of green water phenomenon is carried out by using the dynamic mesh technique.

6.1 Simulation model

In order to study the influence of heave and pitch motion on green water incident, we chose the model used in chapter 5 and compared with the results in given chapter 5. Besides the parameters in Gerco's experiments, we assumed that moment of inertia in y direction I_{yy} was $50\,\mathrm{kg}\cdot\mathrm{m}^2$ and position of gravity center G in vertical direction (the base line is water line) was -0.074m.

6.2 Dynamic mesh

For numerical simulations of moving body or boundary in fluid flow field, dynamic

mesh capability is a common method among the CFD techniques. The dynamic mesh model within ANSYS FLUEMT makes use of three dynamic mesh schemes called smoothing, layering, and remeshing. For these schemes, the layering scheme is always chosen to tackle the problem of purely linear boundary motion; if the relative motions of boundaries are small, we would like to use the spring smoothing to resolve the problem; however; if the relative motions of boundaries are large and general (both translation and rotation may be involved), we need to remesh locally. Most challenging problems of dynamic mesh can be solved by combining these three schemes. Thus, we chose the combination of smoothing and remeshing schemes to simulate the FPSO's heave and pitch motions.

6.2.1 Mesh layout

To ensure proper comparisons between fixed FPSO and moving FPSO, we adopted the same dimensions of numerical wave tank, regional division and wave parameters given in chapter 5. Because the ship heave and pitch motions are simulated by using the dynamic mesh capability, one should consider to model reasonable dynamic grids and to mesh different zones obeying the rules given in chapter 5. According to the motion characteristics of a floating body, we divided the working zone into two different computation zones called static computation zone and dynamic computation zone in order to realize the green water simulation of a moving FPSO.

As can be seen in figure 6.1, the big rectangle around the FPSO is the dynamic computation zone which consists of dynamic computation zone I and II. The meshes in dynamic computation zone I (the small rectangle around the FPSO) are defined as rigid grids. In this zone, all grids are structured meshes, have translation as well as rotation with the FPSO and have no relative motion with respect to the FPSO.

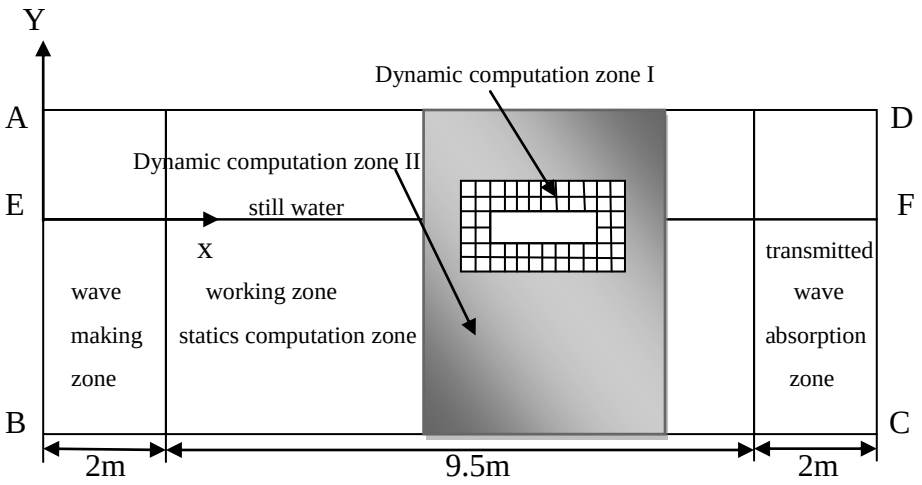

Figure 6.1 FPSO in numerical wave flume

The meshes

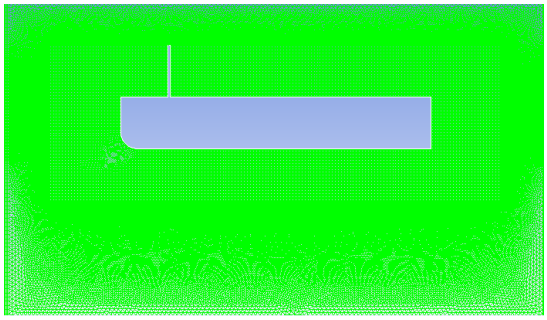

The meshes

Figure 6.2 Mesh layout of moving FPSO model

However, the grids in dynamic mesh zone II are unstructured meshes and will deform with the FPSO motions. For the region near the adjacent boundaries of these two dynamic computation zones, it requires much refined grids in order to get smooth free surface and avoid computational divergence error. The other zones displayed in figure 6.1 should be meshed obeying the rules in chapter 5. The

significance of this regional division is to ensure FPSO motions of arbitrary amplitude and to avoid excessive stretch and distortion, therefore, the computational accuracy and efficiency can be improved. In these simulations, only the heave and pitch motions of the FPSO were considered. Figure 6.2 shows the meshes of the whole domain and the meshes of the dynamic computational domain.

6.3 Boundary conditions and Solver Setups

The same boundary conditions and solver setups as in chapter 5 were adopted in the green water simulation for the moving FPSO.

6.4 Validation and Analysis

To simulate the green water of a moving FPSO model, firstly, the mesh problem has been resolved in section 6.2. After that, based on the method given in chapter 2, the response amplitude operators of the FPSO in different frequencies were calculated. All the parameters and setups used in the numerical model of the fixed FPSO except dynamic mesh were adopted to simulate green water of a moving FPSO. Finally, the simulation was carried out in the ANSYS FLUENT platform and results were obtained.

6.4.1 Response Amplitude Operator Computation of FPSO

In the green water simulation of moving FPSO, the motions of FPSO were calculated by using Potential Flow theory. The response amplitude operators of heave and pitch motions are shown in table 6.1.

Table 6.1 Response Amplitude Operator

Motion	Expression of RAO	Values of RAO	Phase (degrees)
heave	Z_a/ζ_a	0.336189	237.6809
pitch	$\phi_a/\zeta_a(\text{degrees/m})$	23.61783	347.7798

6.4.2 Physical Phenomenon and Result Analysis

In the green water simulation for the moving FPSO, the heave and pitch motions are activated according to phases when the first wave reaches to the bow of the FPSO. In the simulation, the pressure monitor point on the vertical wall was set in the same place of the fixed FPSO case. The figure 6.3 shows the pressure comparison between the fixed FPSO and moving FPSO. The peak values of pressure for the moving FPSO are larger than those for the fixed FPSO. Thus, we can conclude that the ship motions have significant influence on green water loading. The figure 6.4 displays the instantaneous images of green water occurrence over one wave period. The strongly nonlinear phenomena and ship-wave interactions are more apparent. More

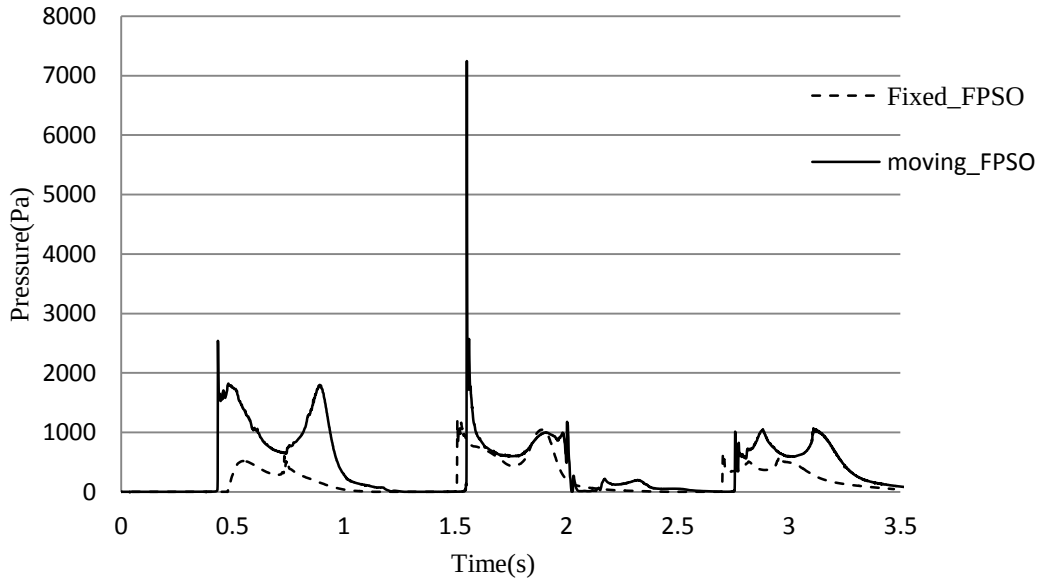

Figure 6.3 Comparison of Green water loading

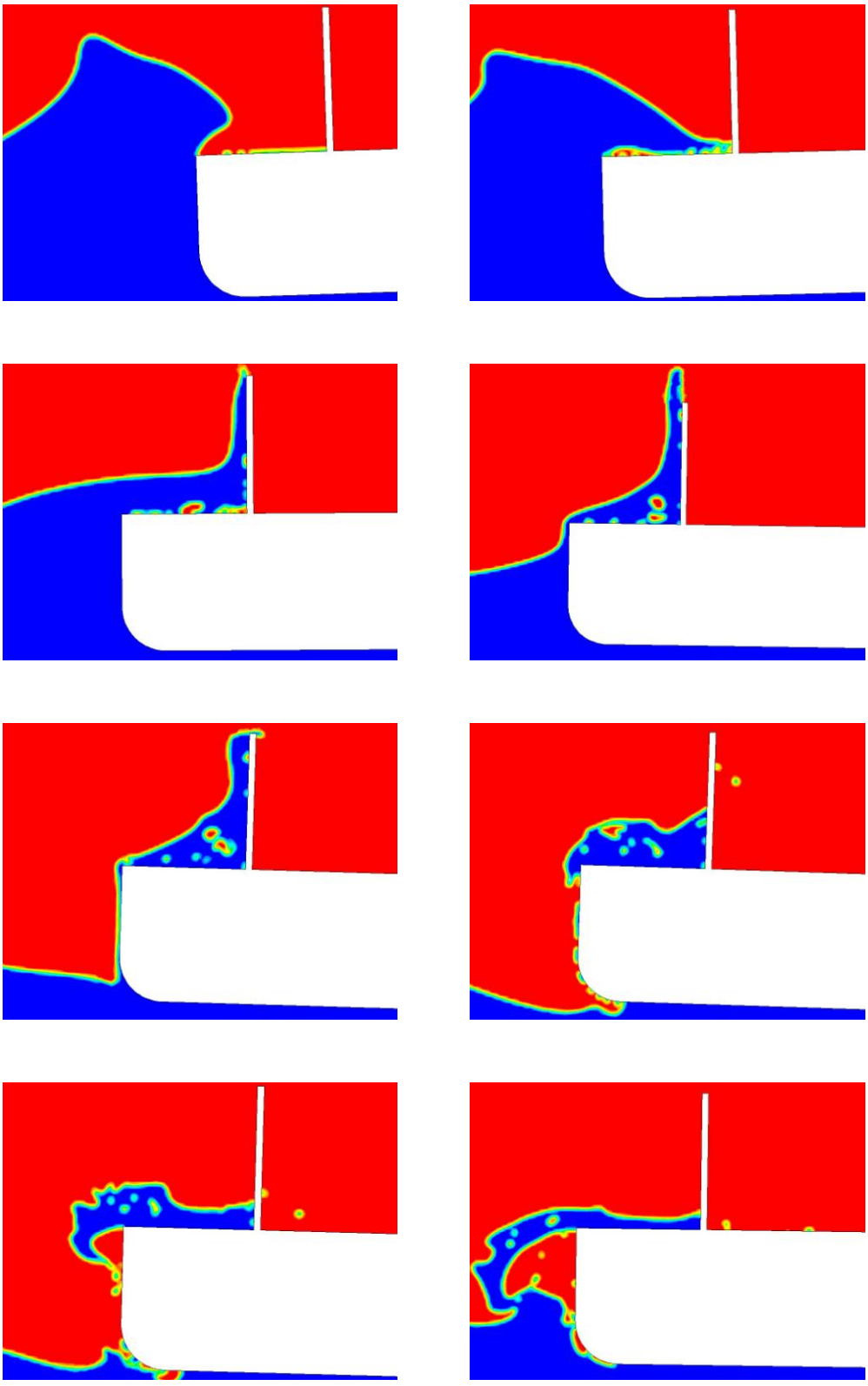

Figure 6.4 Visualization of shipping water on the FPSO deck

importantly, there are two evidences to demonstrate the influence of ship motions' on green water. The first one is that the amount of green water on deck is more than the one in fixed FPSO case. The other one is that the water can overtop the vertical wall in the simulation; however, the vertical wall is high enough to prevent the water overtopping in fixed FPSO case.

6.5 Conclusions

In this chapter, the numerical simulation of green water for moving FPSO (considering heave and pitch motion) was carried out by using ANSYS FLUENT and the green water loading was compared with the fixed FPSO. The comparisons show that the ship motions have significant influences on green water loading. The complicated nonlinear phenomenon can be seen in the simulations.

CHAPTER 7

Summary and Future Perspectives

7.1 Summary

In this thesis, the development history of green water problem was reviewed systematically. A numerical method which takes full advantages of potential flow theory and CFD technique was applied to simulate green water. The complicated physical phenomena of green water can be displayed and the damage to deck structures can be predicted by using this method. Specifically, the green water simulation for fixed ship and moving ship in numerical wave tank can be realized, using continuity and Navier-Stokes equations as control equations, adopting Volume of Fluid (VOF) method to capture the free surface, applying potential flow theory to calculate ship motions and employing dynamic mesh capability to simulate ship motions. Through comparisons with previous experiment, it proved that the present numerical method is a good way to simulate the green water problem. In this thesis, we carried out the green water simulation for fixed and moving FPSOs. These two cases can be summarized as follows:

1. In order to carry out the green water simulations for a fixed FPSO, the numerical model was established based on the Greco's(2001) experiment model. And the accuracy of the computation results was validated via the comparison with the experiments. The significance of the simulations is mainly to study the stages of

wave-ship interaction including the run-up of the water at the bow, the water shipping on the deck, the subsequent flow developing along the deck and the impact on ship equipment or deck structures. The investigation showed that the 2-D numerical model can describe the complicated nonlinear phenomena such as jet flow and wave breaking; the water elevation height on the deck and the impact forces acting on a vertical wall matched well with the experimental measurements.

2. In order to simulate the green water for a moving FPSO, the same FPSO model as in the fixed FPSO case was chosen and the FPSO's heave and pitch motions were taken into account. The impact pressures obtained from the moving FPSO case were compared with the impact pressures on the fixed FPSO's. The comparisons show that ship motions have a great influence on the green water phenomenon. Thus, it indicates that the ship motions should be considered in the future research.

7.2 Future Perspectives

The main research task of the thesis is to carry out the 2-D green water simulation of a FPSO. Although the full use of the advantages of potential flow theory as well as CFD technique were made in the simulations and good results were obtained, there were many simplifications. For example, the FPSO was simplified as a rectangle box and the 3-D effect were not considered in the simulations. Therefore, the establishment of the model of actual ship and the 3-D simulations are the challenges in the future, since the simulations require more precision, higher computational stability and improved dynamic mesh technique.

In the green water simulations of a moving FPSO, the ship motions were calculated

by using the potential flow theory in advance. After the wave reached the bow of FPSO, the ship motions were activated with the corrected phase angles. Therefore, this is unsteady problem. However, as the ship motions were computed in steady waves in the present simulations, the ship motions cannot match very well with the waves. At the same time, there exists a complicated relationship between shipping water and ship motions. The shipping water on the deck and ship motions will influence each other. The further challenge is to calculate the ship motions by Fluent and therefore to achieve the full coupling between waves and ship motions. The establishment of a numerical model which can simulate the full coupling between waves and a floating structure and green water incident is a future research requirement.

References

Buchner, B. (1995a). The Impact of Green Water on FPSO Design. In Offshore Technology Conference 95 (OTC'95). Houston, USA. OTC paper 7698.

Buchner, B. (1995b). On the Impact of Green Water Loading on Ship and Offshore Unit design. In the Sixth International Symposium on Practical Design of Ships and Mobile Units (PRADS'95).

Buchner, B. & Cozijn, J. L. (1997). An Investigation into the Numerical Simulation of Green Water. In Proc. Int. Conf. on the Behaviour of Offshore Structures, BOSS'97, vol. 2, pages 113-125.

Buchner, B. & Voogt, A. (2000). The Effect of Bow Flare Angle on FPSO Green Water Loading. Proceeding of 19th OMAE. New Orleans.

Dai, Y., Shen, J. and Song, J. Ship Wave Loads. National Defense Industry Press, Beijing, 2005.

Dai, Y. Potential Flow Theory of Ship Motion in Waves in Frequency and Time Domain. National Defense Industry Press, Beijing, 1998.

Drake, K. R. (2000). Transient Design Waves for Green-water Loading on Bulk Carriers. Journal of Marine Science Technology, pages 21-30.

Ersdal, G. & Kvitrud, A. (2000). Green Water on Norwegian Production ships. In Proceedings of Tenth (2000) International Offshore and Polar Engineering Conference, pages 211-218. Seattle, USA.

Faltinsen, O. M., Greco, M. & Landrini, M. (2002). Green Water Loading on FPSO, Journal of Offshore Mechanics and Arctic Engineering, 124, pages 94-103.

Faltinsen, O. M. (1990). Sea Loads on Ships and Offshore Structures. Cambridge University Press.

Faltinsen, O, M. (2005). Hydrodynamics of High-speed Marine Vehicles. Cambridge University Press.

Fekken, G., Veldman, A. E. P. & Buchner, B. (1999). Simulation of Green Water Loading Using the Navier-Stokes Equations. In seventh International Conference on Numerical Ship Hydrodynamics. Nantes.

Goda, K., Miyamoto, T. & Yamamoto, Y. (1976). A Study of Shipping Water Pressure on Deck by Two Dimensional Ship Model Test. Journal of the Society of Naval Architects of Japan, vol.140.

Greco, M., Faltinsen, O. M. & Landrini, M. (2000). Basic Studies of Water on Deck. 23rd Symposium on Naval Hydrodynamics. Val de Reuil, France, September 2000.

Greco, M., Faltinsen, O. M. & Landrini, M. (2001). Green Water Loading on A Deck Structure. Proceedings, 16th International Workshop on Water Waves and Floating Bodies, April, Hiroshima, Japan.

Greco, M. (2001). A Two-dimensional Study of Green-Water Loading. PHD thesis, Norwegian University of Science and Technology, Trondheim, Norway.

Hamoudi, B. & Varyani, K. S. (1998). Significant Load and Green Water on Deck of Offshore Units/Vessels. Ocean Engineering, 25(8), pages 715-731.

Han, JuChull (2003). Impact of Green Water on FPSOs. PHD thesis, University of Newcastle upon Type.

Larsen, J., Dancy, H. (1983). Open Boundary in Short-wave Simulation—a New Apporoach. Costal Engineering, 285-297.

Makoto, A. & Uttam, K. P. (1993). A Technique for Open Boundary Treatment in Numerical Wave Tanks. Journal of The Society of Naval Architects of Japan, vol.173, 45-50.

Nielsen, K. B. & Mayer, S. (2004). Numerical Prediction of Green Water Incidents. Ocean Engineering, 31, pages 363-399.

Ochi, M. K. (1964). Extreme Behavior of A Ship in Rough Seas. Annual Meeting of the Society of Naval Architects and Marine Engineering, pages 143-202.

Pham, X. P. & Varyani, K. S. (2005). Evaluation of Green Water on High-speed Containership Using CFD. Ocean Engineering, 32(5-6), pages 571-585.

Renchuan Zhu, Guoping Miao and Zhaowei Lin (2009). Numerical Research on FPSOs With Green Water Occurrence. Journal of Ship Research, Vol. 53, No.1, pp. 7-18.

Salvesen, N., Tuck, E. O., & Faltinsen, O. M. (1970). Ship Motions and Sea Loads. Trans. SNAME, 78,250-87.

Stansby, P. K., Chegini, A. & Barnes, T. C. D. (1998). The Initial Stages of Dam-break Flow. Journal of Fluid Mechanics, vol. 374, pages 407-424.

Stansberg, .C T. & Karlsen, S. I. (2001). Green Sea and Water Impact on FPSO in Steep Random Waves. In Practical Design of Ships and Other Floating Structures (PRADS 2001), Shanghai, China.

Tan, S. G. (1969). Observations Made on Board Dutch Merchant ships. International shipbuilding Progress, vol.16 (181): pages 259-276.

Touze, D. Le., Marsh, A., Oger, G., Guilcher, P. M., Khaddaj-Mallat, C., Alessandrini, B. & Ferrant, P. (2010). SPH Simulation of Green Water and Ship Flooding Scenarios. Ninth International Conference on Hydrodynamics, October 11-15, Shanghai, China.

Vermeer, IR. H. (1980). Prediction of the Amount of Shipping Water. Rep. of the Netherlands Maritime Institute, pages 3-21.

Wang, B. L. & Liu, H. (2005). Higher order Boussinesq-type equations for water waves on uneven bottom. Applied Mathematics and Mechanics, 26, 6, 714-722.

Yamasaki, J., Miyata, H. & Kanai, A. (2005). Finite-difference Simulation of Green Water Impact on Fixed and Moving Bodies. Journal of Marine Science and Technology, 10(1), pages 1-10.

Yilmaz, O., Incecik, A. & Han, J. C. (2003). Simulation of Green Water Flow on Deck using Non-linear Dam Breaking Theory. Journal of Ocean Engineering, 30 (5), pages 601-610.

AQWA™-LINE MANUAL. Copyright 2006, Century Dynamics Limited.

ANSYS (Release 13.0) FLUENT Theory Guide. ANSYS, Inc. November 2010.

ANSYS (Release 13.0) FLUENT UDF Manual. ANSYS, Inc. November 2010.